Diving into the Molecular Diversity of Aplysina cavernicola's Exometabolites: Contribution of Bromo-Spiroisoxazoline Alkaloids

Morgane Mauduit, Stéphane Greff, Gaëtan Herbette, Jean-Valère Naubron, Sara Chentouf, Trung Huy Ngo, Joo-Won Nam, Sacha Molinari, Fathi Mabrouki, Elnur Garayev, et al.

ACS OMEGA

http://pubs.acs.org/journal/acsodf

Article

Diving into the Molecular Diversity of *Aplysina cavernicola's* Exometabolites: Contribution of Bromo-Spiroisoxazoline Alkaloids

Morgane Mauduit, Stéphane Greff, Gaëtan Herbette, Jean-Valère Naubron, Sara Chentouf, Trung Huy Ngo, Joo-Won Nam, Sacha Molinari, Fathi Mabrouki, Elnur Garayev, Béatrice Baghdikian, Thierry Pérez, and Charlotte Simmler*

Cite This: *ACS Omega* 2022, 7, 43068–43083

Read Online

ACCESS | Metrics & More | Article Recommendations | Supporting Information

ABSTRACT: Sponges are prolific producers of specialized metabolites with unique structural scaffolds. Their chemical diversity has always inspired natural product chemists working in drug discovery. As part of their metabolic filter-feeding activities, sponges are known to release molecules, possibly including their specialized metabolites. These released "Exo-Metabolites" (EMs) may be considered as new chemical reservoirs that could be collected from the water column while preserving marine biodiversity. The present work aims to determine the proportion and diversity of specialized EMs released by the sponge *Aplysina cavernicola* (Vacelet 1959). This Mediterranean sponge produces bromo-spiroisoxazoline alkaloids that are widely distributed in the Aplysinidae family. Aquarium experiments were designed to facilitate a continuous concentration of dissolved and diluted metabolites from the seawater around the sponges. Mass Spectrometry (MS)-based metabolomics combined with a dereplication pipeline were performed to investigate the proportion and identity of brominated alkaloids released as EMs. Chemometric analysis revealed that brominated features represented 12% of the total sponge's EM features. Consequently, a total of 13 bromotyrosine alkaloids were reproducibly detected as EMs. The most abundant ones were aerothionin, purealidin L, aerophobin 1, and a new structural congener, herein named aplysine 1. Their structural identity was confirmed by NMR analyses following their isolation. MS-based quantification indicated that these major brominated EMs represented up to 1.0 ± 0.3% w/w of the concentrated seawater extract. This analytical workflow and collected results will serve as a stepping stone to characterize the composition of *A. cavernicola's* EMs and those released by other sponges through *in situ* experiments, leading to further evaluate the biological properties of such EMs.

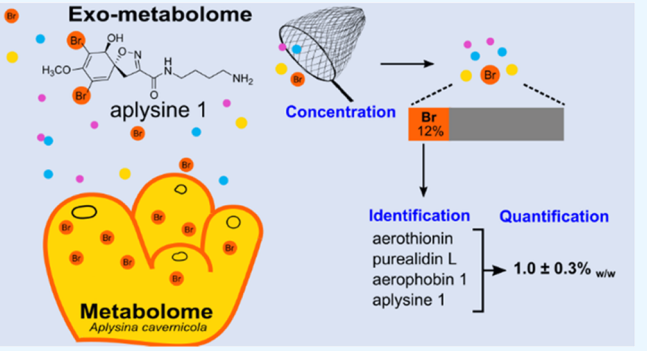

INTRODUCTION

Sponges (Phylum Porifera) are sessile aquatic animals that live on diverse substrates at the bottom of the seas, mangroves, lakes, and rivers. They are one of the most complex holobionts, often defined as meta-organisms encompassing the eukaryotic host and its associated highly diverse microbiota.[1] Representing up to 60% of the sponge biomass, such microbiota contributes to the host nutrition, defense, and overall metabolic activities. As stated by Pita et al., sponges as holobionts perform functions that cannot be accomplished by the partners (*e.g.*, microsymbionts) separately.[1] Such functions notably involve the production of structurally complex molecules often called specialized metabolites participating in the sponge defense against pathogens, predators, and other species competing for space.[2−6] The chemistry of sponge-specialized metabolites has been extensively studied by natural product chemists working in drug discovery mainly in the fields of cytotoxic/anticancer and antimicrobial research.[7−10] Nowadays, marine sponges remain one of the most prolific sources of molecules harboring original structural scaffolds. Approximately 200 new molecules reported each year,[10,11] leading to an estimate of >7000 compounds isolated from sponges since the beginning of research on marine natural products in the 1960s. Clearly, the chemodiversity of sponges is an important source of inspiration for chemists and biologists. Traditionally, the biological evaluation of sponge metabolites requires the harvesting of large quantities of biomass, which significantly impacts marine ecosystems. In the actual context of a biodiversity crisis facing a changing environment, there is a need to develop ecoresponsible approaches maintaining access to sponge chemodiversity while preserving marine biodiversity. Such approaches need to

Received: August 23, 2022
Accepted: October 26, 2022
Published: November 16, 2022

Scheme 1. General Workflow to Study the Diversity and Quantity of Brominated Specialized Metabolites Released by the Sponge *A. cavernicola*

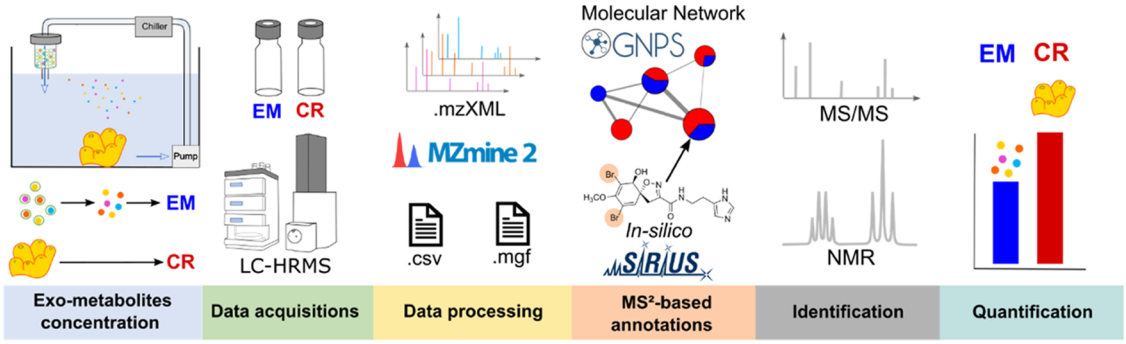

integrate knowledge and expertise in sponge biology, marine ecology, and natural product chemistry.

Marine sponges can be abundant both in terms of species diversity and biomass in various benthic habitats. They are also one of the most efficient filter feeders participating in the functioning of marine ecosystems notably through benthic-pelagic couplings, i.e., the exchanges of nutrients between the bottom of the ocean (benthos) and the water column (pelagos).[12−14] Sponges feed on suspended organic material (eubacteria, cyanobacteria, nanoeukaryotes, detritus)[15] and actively contribute to the recycling of particulate and dissolved organic matters (POM and DOM) produced by many other marine organisms. This function also leads to a subsequent release of new molecules, either dissolved or associated with particulates (*e.g.*, sponge cellular debris). Such released molecules are derived from the holobiont biosynthetic potentials and from the biotransformation of food. All molecules released by sponges in their surroundings are, herein, called Exo-Metabolites and abbreviated EMs in the manuscript. Upon their release by the sponges, these EMs may be diluted in the aqueous environment as a function of their water solubility and mixed with other EMs from marine organisms. Part of these EMs can serve as chemical cues influencing the behaviors of marine organisms, thus also participating in the functioning of ecosystems, as demonstrated previously.[16,17]

Pooled EMs issued from different marine organisms constitute chemical seascapes made of thousands of distinct molecules in trace amounts (ppm, mg/L), often summarized as marine DOM.[18−21] Due to their complexity, the composition of chemical seascapes has been barely explored.[18,19] Therefore, as suggested by Kelly et al.,[20] characterizing the molecular diversity of discrete source of marine EM will help not only to decipher the complexity of each chemical seascape but also to identify the ecological functions related to specific EM and possibly uncover new metabolites with biological potentials. Targeted studies performed with a few sponge species (namely, *Aplysina fistularis*,[22] *Agelas conifera*,[23] *Aplysilla rosea*,[24] and also *Crambe crambe*[25,26]) revealed that some of their specialized metabolites could be detected in the surrounding seawater. This information also suggests that sponge exometabolomes can represent unique reservoirs of structurally diverse molecules, potentially including their bioactive specialized metabolites. Collected from the water column surrounding the sponges without altering their biomass, such specialized EMs could become a new source of inspiration in drug discovery. However, studying the chemical and biological potentials of sponge's EMs requires a variety of technical challenges to be addressed, the first one being the concentration of molecules in a diluted aqueous environment. The second encompasses the identification and quantification of molecules in a complex mixture. Moreover, due to the lack of available mass spectrometry (MS) data from marine organisms in public databases, less than 10% of marine metabolites can be annotated.[20,21] Such situations require targeted isolation of already known metabolites to confirm their structural identity and/or the use of *in silico* structural annotation tools such as SIRIUS MS/MS or CFM-ID.[20,27,28]

The present study proposes an experimental workflow (Scheme 1) to overcome the listed technical challenges and evaluate the proportion and identity of specialized metabolites released in seawater from a sponge species harboring structurally known and potentially bioactive metabolites. Therefore, *Aplysina cavernicola* (Vacelet 1959) was selected as a model in our study as this sponge is (1) particularly abundant in Mediterranean benthic habitats (Figure S1)[29] and (2) a well-known producer of structurally diverse brominated spirocyclohexadienyl-isoxazoline (abbreviated bromo-spiroisoxazoline) alkaloids that are also detected in closely related species of the same Aplysinidae family distributed worldwide. As such, the compound aerothionin is the most abundant of all of these alkaloids in *A. cavernicola* and is distributed widely in other species within the Aplysinidae family and the Verongida order.[30−38] This compound was found to be released in seawater by the Caribbean sponge *A. fistularis* with and without application of wound-induced stress.[22] Other bromotyrosine derivatives of smaller molecular weight (*e.g.*, aeroplysinin-1 or aplysamine-1) are also reported to be produced by closely related *Aplysina* species.[39,40] In terms of biological evaluation, most of these compounds have been reported to have antimicrobial and/or antifouling properties.[41,42] Finally, the characteristic MS isotopic pattern of bromine (Br) facilitates the detection of *A. cavernicola* specialized metabolites even when present in trace quantities as EMs.

The work presented herein with *A. cavernicola* aims to (1) determine whether brominated alkaloids, possibly other than aerothionin, can be detected as EMs (2) evaluate the proportion of those specialized EMs with regard to the overall chemical composition and diversity of *A. cavernicola* exometabolome, and (3) quantify those identified brominated EMs in the concentrated seawater extract and around the sponge. Starting with the capture and concentration of sponge EMs from the seawater, the proposed workflow relies on MS-based metabolomics, dereplication by molecular networking,[43] eventually complemented by *in silico* structural annotation. Target isolation of brominated alkaloids from the sponge biomass was performed whenever possible to confirm their structural identity and enable their quantification when detected as EM.

https://doi.org/10.1021/acsomega.2c05415
ACS Omega 2022, 7, 43068−43083

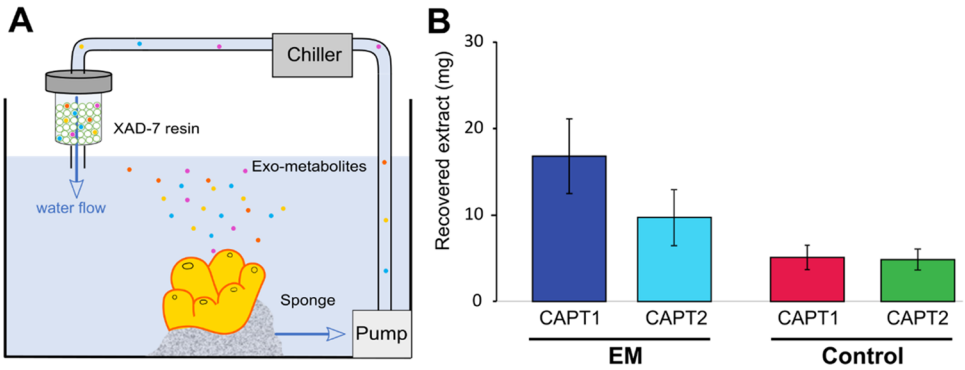

Figure 1. (A) Scheme of the aquarium setup for the concentration of exometabolites (EMs, colored dots) on XAD-7 resins. (B) Average quantity of recovered extracts after 16-h capture of sponge EMs compared to other seawater metabolites for CAPT1 and CAPT2 (mean ± standard deviations of three measurements).

RESULTS AND DISCUSSION

Continuous Adsorption of Exometabolites in Aquaria. In this study, we designed aquarium experiments to work in a controlled environment, using defined volumes of seawater (50 L) and quantities of sponge biomasses (~100 cm^3), thereby allowing us to quantitatively evaluate the release of specialized metabolites over time (Figure 1A). Adsorption and concentration of dissolved metabolites in aqueous media are generally performed using solid-phase extraction cartridges, disks, or polymeric resins (*e.g.*, Amberlite XAD).[16,21,26,44−46] These techniques are widely used to concentrate organic environmental pollutants from water.[47,48] *In situ* continuous and passive adsorption of metabolites from aqueous media is generally performed using polymeric resins.[25,26,45,47,49] As such, the resins XAD-7 and XAD-16 were used to adsorb metabolites released in an aquarium by the sponges *Aplysilla rosea*[24] and *Crambe crambe*,[26] respectively. In line with these studies, we developed our aquarium experiments using XAD-7, filled in an external cartridge directly connected to the aquarium pump (Figure 1A). Such resin was found to offer similar adsorption affinities for bromo-spiroisoxazolines as XAD-16 (Figure S2). All experiments were performed with *A. cavernicola* specimens collected with their rocky substrate and after a minimum of 24 h of acclimation in the aquarium with continuous renewal of natural seawater. Each adsorption experiment was performed for a 16-h period in a closed water circuit. The unidirectional water flow through the cartridge filled with XAD-7 favors a continuous adsorption of EMs while avoiding their local concentration around the sponges. Water movement was therefore maintained in the aquarium. The purpose of such a setup was to enable a rapid capture of EMs upon their release and progressively increase the quantity of such metabolites adsorbed on the XAD-7 resin. Between each period of adsorption, natural seawater was renewed in the aquarium continuously and for a minimum of 8 h. Each cycle of adsorption was repeated three times for each sponge sample collected independently in November 2020 (CAPT1) and May 2021 (CAPT2). Sponge health status was regularly monitored before and after each adsorption period to check, *e.g.*, the persistence of the biomass yellow coloration and the opening of oscula.

The collected resins from each of the adsorption experiment were eluted with 100% MeOH to recover the EMs. Extracts thereby obtained were abbreviated EM1−3 and differentiated between CAPT1 and CAPT2. For each adsorption experiment, the exact same aquarium setup was performed without a sponge, thus leading to the production of extracts containing all seawater metabolites, except those produced by the sponges. Such extracts were used as analytical controls. At the end of the experiments, sponges from CAPT1 and CAPT2 were flash frozen, freeze-dried, and extracted with 100% MeOH, leading to the production of crude extracts serving as analytical references for the dereplication of brominated alkaloids. The recovered EM extracts accounted for 16.8 ± 4.2 mg for CAPT1 and 9.7 ± 3.2 mg for CAPT2, whereas the total amount of recovered seawater control extracts totaled 5.8 ± 1.4 mg for CAPT1 and 4.8 ± 1.2 mg for CAPT2 (Figure 1B).

Metabolite Profiling and Detection of Brominated Features in Exometabolomes. Untargeted Liquid Chromatography−Mass Spectrometry (LC−MS)-based metabolomic analysis was implemented to compare the composition of replicate extracts (EM, crude, controls) from both CAPT1 and 2. The objectives were to (1) assess the overall differences in exometabolite composition between EM and control extracts and, (2) evaluate the chemical similarities between EM and crude extracts by determining the presence of brominated features (Figure 2). A principal component analysis (PCA) was first performed with the MS^1 data matrix exported from MZmine 2.53 and containing 2508 chemical features (Figure 2A). On the score plot, each set of extract replicates occupies a distinct chemical space. Permanova analysis [Classification Error Rate (CER) = 0.058, *p*-value = $9.999e^{-5}$] indicated that all groups of extracts are statistically different from each other, thereby suggesting a unique composition of recovered exometabolites associated with the metabolic activities of the sponges. This first observation agrees with previous reports demonstrating that sponges change the composition of their surrounding seawater through their metabolic filter-feeding activities.[50,51] Nevertheless, for both CAPT1 and 2, EM and control extracts were statistically more similar than EM and crude extracts, especially along PC1 (19.9% of variance). This result indicates that EM extracts shared more chemical information with control extracts than with their sponge crude extracts, both in terms of diversity and intensity of detected chemical features.

A Partial Least-Square Discriminant Analysis (PLS-DA) was then performed to extract variable importance in projection (VIP) with scores >1. The objective was to facilitate the detection of key discriminant brominated features present in both crude and EM, but not in control extracts (Figure 2B). By analyzing the top 30 among the 655 VIP with scores >1, a total of 17 features were found to be present in both EMs and crude only. After further MS^1 data inspections, characteristic brominated isotopic patterns were detected for 16 of the 17

https://doi.org/10.1021/acsomega.2c05415
ACS Omega 2022, 7, 43068−43083

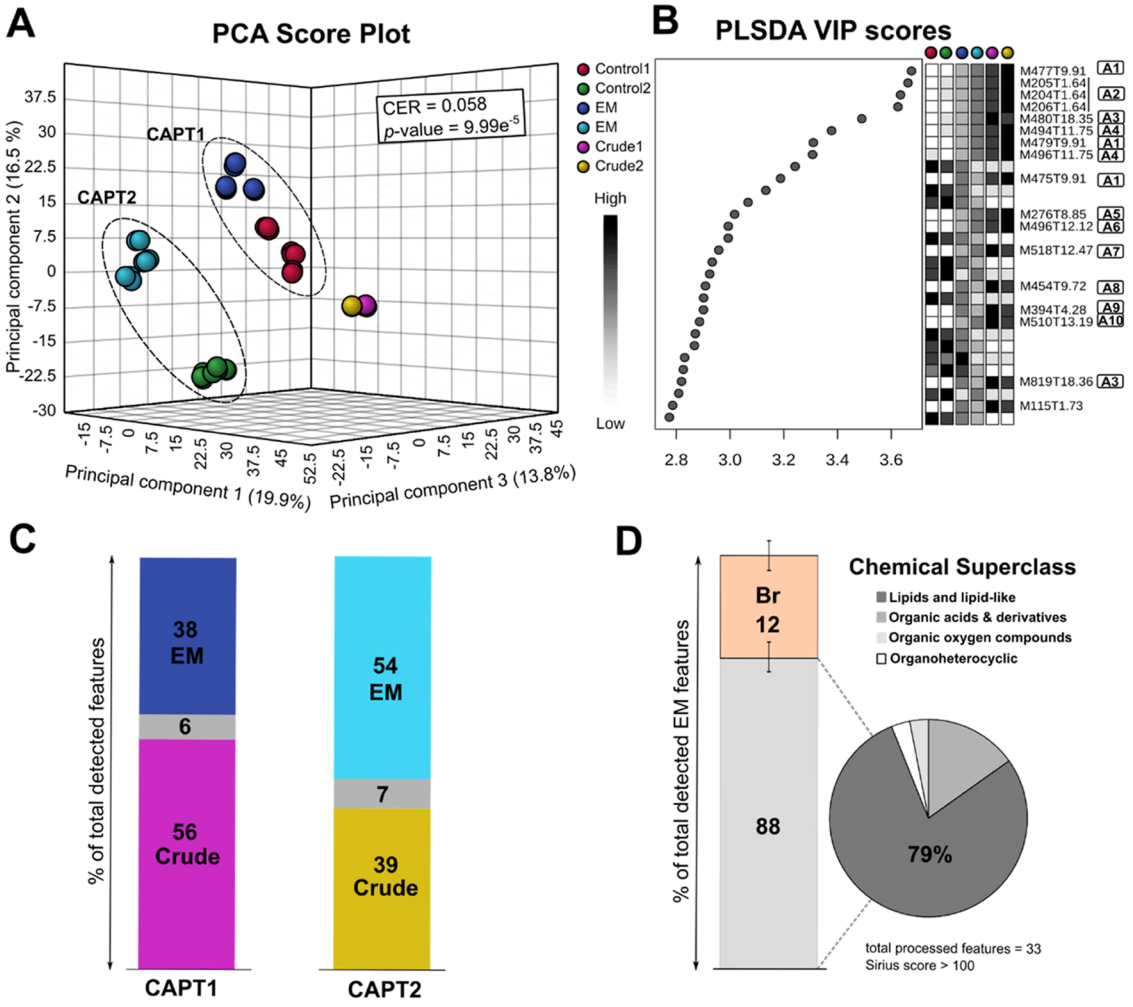

Figure 2. (A) Principal component analysis (PCA) score plot showing that *A. cavernicola* crude, the sponge's exometabolites (EMs), and seawater control extracts occupy distinct chemical space. CER stands for Classification Error Rate. (B) Partial Least-Square Discriminant Analysis (PLS-DA) variable importance in projection (VIP) scores taking the top 30 discriminant features along component 1 (19.9% variance) highlighting key brominated features codified **A1**−**A10** (*M* = measured *m*/*z*, *T* = retention time in min) detected in both crude and EM extracts. (C) Bar graphs representing the distribution of chemical signals between crude and EM extracts, expressed as a percentage of total detected features. The gray zone represents the proportion of features detected in both crude and EM extracts. (D) Proportion of detected brominated, **Br**, signals in the sponge's EM extracts and expressed as a percentage of the total detected EM features for CAPT1-2. Repartition of the chemical diversity of non-brominated EMs within the recovered extracts. The gray pie chart represents the proportion of features detected reproducibly in CAPT1 and CAPT2 and annotated in structural superclass using CANOPUS.[51]

discriminant features. To avoid chemical redundancy, the *m*/*z* values of features defined by identical retention time and corresponding to (1) bromine isotopic pattern, and (2) in-source fragments of the same brominated molecule were combined to keep only molecules associated with their monoisotopic $[M + H]^+$ molecular ion. Such brominated metabolites detected in both crude and EM extracts were codified (**Ax**). As such, the feature M480T18.35 (monoisotopic *m*/*z* 479.9599 $[C_{15}H_{17}Br_2N_3O_5 + H]^+$) was detected at the same retention time than M819T18.36 (monoisotopic *m*/*z* 814.8571 $[C_{24}H_{26}Br_4N_4O_8 + H]^+$) and corresponded to the in-source fragment along with the parent ion of aerothionin **A3**, as described by Nicacio et al.[52] The feature M115T1.73 did not exhibit a brominated characteristic pattern, and thus, was not codified (Figure 2B). These first results revealed that several brominated metabolites, such as aerothionin **A3**, were recovered from the seawater around *A. cavernicola*. The next objective was therefore to determine the total proportion of released brominated features within the sponge's exometabolome.

Proportion of Brominated Features in A. cavernicola's Exometabolome. To determine the proportion of features that are shared between crude and EM extracts in the entire dataset, we evaluated the general distribution of chemical features detected in crude and in each of the three EM extracts for CAPT1 and CAPT2 by analyzing the MS^1 data matrix. Features detected in controls were discarded from the analysis. As represented in Figure 2C, features present in both crude and EM extracts, possibly encompassing sponge-specialized brominated metabolites, accounted for 6% of the total detected features in CAPT1 and 7% in CAPT2. Interestingly, the proportion of shared features between crude and EM extracts was very similar for both CAPT1 and CAPT2, as opposed to the proportion of features specifically detected in EM or crude. Such a result suggested that the proportion of brominated specialized metabolites reproducibly released may be constant for a given sponge biomass.

The second step was to determine the proportion of detected brominated features in the EMs (Figure 2D). The MS^1 data

https://doi.org/10.1021/acsomega.2c05415
ACS Omega 2022, 7, 43068−43083

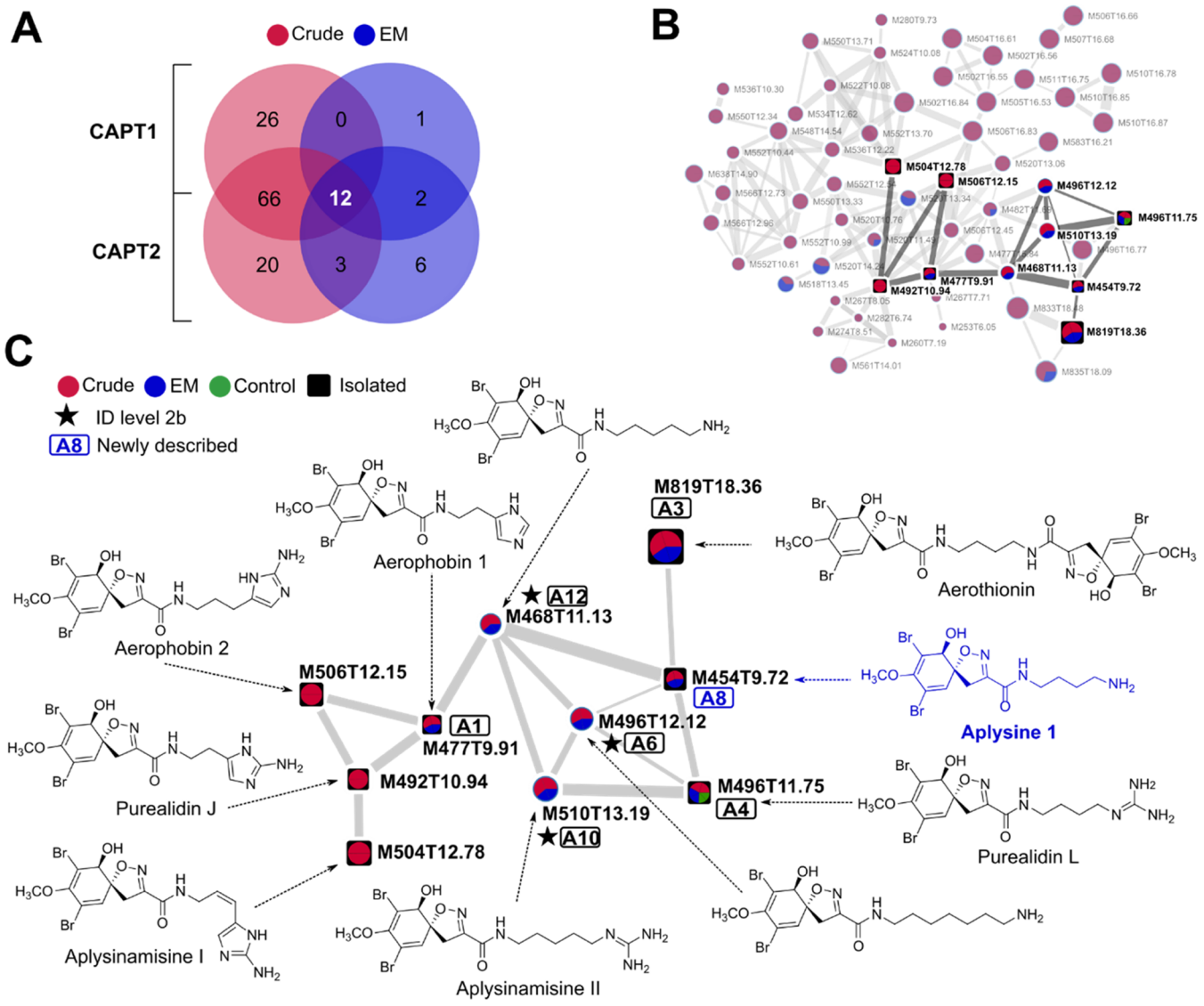

Figure 3. (A) Venn diagrams of brominated alkaloids detected in crude (red) and EM (blue) extracts for both CAPT1 and 2. 12 brominated metabolites were reproducibly detected in crude and EMs. (B) Feature-based molecular network of the bromo-spiroisoxazoline spectral family including 61 nodes designed by their M = measured m/z of precursor ion and T = retention time (min). Each node corresponds to one compound. The size of the node is proportional to the retention time. The pie chart represents log-transformed ion intensities of the corresponding molecule in different extracts. (C) Focus on connected nodes used for the dereplication. Molecules **A1**, **A3**, **A4**, **A6**, **A8**, **A10**, and **A12** were detected in both crude and EM extracts. Structures **A6, A10**, and **A12** are proposed with a level 2B of confidence[62] based on the comparative analysis of their MS^2 spectra with that of **A8**.

matrix of all EM samples was inspected to select features with characteristic brominated isotopic pattern. A total of 23 brominated signals were found in CAPT1 EMs (among 215 signals) and 39 in CAPT2 EMs (among 333 signals), thereby collectively representing 12% of all detected features in EMs. Hence, the majority of recovered EM features (88%) were not brominated. Only 20% of those non-brominated features, accounting for a total of 83 features, were reproducibly detected in all EM replicates for CAPT1 and CAPT2. To explore their molecular diversity, these features were further analyzed using SIRIUS MS/MS annotation tools[28] to predict their molecular formula and gain insights as per their distribution in structural classes. Signals associated with noisy MS^2 data precluding accurate structural analysis, and harboring Sirius scores <100 were discarded. Following this data treatment, using CANOPUS,[51] the majority of exometabolites (79%) were found to belong to the superclass of lipids and lipid-like molecules. The remaining exometabolites were distributed between the superclasses of organic acids and derivatives (15%), organoheterocyclic (3%) and organic oxygen (3%) compounds. Such structural distribution of EM features follows a pattern similar to what has been recently published on the chemical diversity of other marine exometabolomes.[20,51,53] Part of these exometabolites could originate from bacterial (microsymbiont) metabolism, as well as sponge cellular metabolic waste and dissolution of lipids from disrupted cellular detritus to cite a few examples.[20,51,54]

MS-Based Annotation and Identification of Brominated Exometabolites. Despite their lower proportion in *A. cavernicola's* EMs, the released brominated metabolites with higher VIP scores mainly participate in the differentiation of EMs from controls. To confirm the identity of the detected

https://doi.org/10.1021/acsomega.2c05415
ACS Omega 2022, 7, 43068−43083

Table 1. ESI-MS^2 Data of Identified or Annotated Bromotyrosine Spiroisoxazolines Present in the Sponge Extract and Reproducibly Detected as EMs

common name	code (cluster index)[a]	RT (min)	molecular formula	ion status	measured[c]	calculated[c]	MS^2 fragments & intensities[d]		ID[e]
					m/z				
A1 aerophobin 1	M477T9.91 **(5)**	9.91	$C_{15}H_{16}Br_2N_4O_4$	$[M + H]^+$	474.9611	474.9611	95.0604 138.0665 165.0775 **294.8790**	100.0 60 13.3 18.7	1
A2 aplysamine 1	M205T1.64 **(4)** M409T1.63 **(42)**[b]	1.64	$C_{15}H_{24}Br_2N_2O$	$[M + 2H]^{2+}$ $[M + H]^+$	204.0203 407.0353	204.0200 407.0334	58.0651 86.0963 168.9645 320.9357	100.0 8.3 4.5 4.3	2b
A3 aerothionin	M819T18.36 **(21)**	18.36	$C_{24}H_{26}Br_4N_4O_8$	$[M + H]^+$	814.8555	814.8557	98.0601 115.0868 **294.8786** 479.9587	41.8 16.4 100.0 51.8	1
A4 purealidin L	M496T11.75 **(3)**	11.75	$C_{15}H_{21}Br_2N_5O_4$	$[M + H]^+$	494.0031	494.0033	98.0602 114.1026 157.1081 200.1143 **294.8792**	47.5 11.7 40.8 20.0 23.3	1
A5	M276T8.85 **(23)**[b]	8.85	$C_{19}H_{32}Br_2N_6O_3$	$[M + 2H]^{2+}$	275.045	275.0446	58.0648 157.1082 184.1196	100.0 60.9 32.6	-
A6 aplysine 1 congener	M496T12.12 **(20)**	12.12	$C_{17}H_{25}Br_2N_3O_4$	$[M + H]^+$	494.0282	494.0285	114.1279 157.1337 200.1394 **294.8787**	73.3 93.3 20.7 15	2b
A7	M518T12.49 **(167)**[b]	12 .49	$C_{16}H_{15}Br_2N_5O_5$	$[M + H]^+$	515.9516	515.9513	136.0508 179.0537 206.0679 **294.8786**	100.0 31.3 58.1 30.3	2b
A8 aplysine 1	M454T9.72 **(22)**	9.72	$C_{14}H_{19}Br_2N_3O_4$	$[M + H]^+$	451.9821	451.9815	55.0540 72.0805 98.0601 115.0867 **294.8788** 319.8743 436.9536	24.5 80.0 100.0 85.0 65.0 11.5 15.0	1
A9	M392T4.28 **(94)**[b]	4.28	$C_{12}H_{11}Br_2NO_4$	$[M + H]^+$	391.9104	391.9128	N	N	-
A10 aplysinamisine II	M510T13.19 **(33)**	13.19	$C_{16}H_{23}Br_2N_5O_4$	$[M + H]^+$	508.0181	508.0190	86.0962 112.0758 171.1239 214.1296 **294.8786**	21.5 75.4 100.0 29.2 29.2	2b
A11 aeroplysinin-1	M340T4.28 **(76)**	4.28	$C_9H_9Br_2NO_3$	$[M + H]^+$	337.9023	337.9022	121.0285 135.0443 187.9652 213.9625 241.9578 **294.8792**	15.5 30.9 53.6 100.0 84.5 90.9	1
A12 aplysine 1 congener	M468T11.13 **(66)**	11.13	$C_{15}H_{21}Br_2N_3O_4$	$[M + H]^+$	465.9966	465.9972	69.0696 86.0963 112.0759 129.1022 **294.8786** 332.8574	12.5 58.4 45.5 100.0 49.4 8.2	2b

[a]The cluster index identifies nodes in the GNPS molecular network, the most intense peak of the isotopic pattern was used for feature codification. [b]Single node. [c]The monoisotopic peak was selected for molecular formula determination. [d]Major MS^2 fragments and their intensities were selected using the GNPS Metabolomics USI tool. N = noisy MS^2 spectra. [e]Confidence level of metabolite identification according to Schymansky et al.[62] See Supporting Information S6.

brominated exometabolites, a Feature-Based Molecular Network (FBMN)[43] was performed in the GNPS environment using the exported spectra files (.mgf) and feature list (.csv) from MZmine 2.53.[55] The generated molecular network was processed and visualized using Cytoscape 3.8.[56] The chemical features represented as nodes are grouped according to the similarity of their MS^2 spectra, which facilitate the dereplication process toward the annotation of representative *A. cavernicola* metabolites. Log-transformed relative ion intensities within the set of samples were used to represent each node/feature with a color-coded pie chart (Figures 3, 4 and S4). All brominated features of interest were distributed in three spectral families. Both .mgf and .csv files were cleaned to remove isotopes and in-source fragments, leading to a total of 127 brominated metabolites found in the set of sponge crude extracts and 78 of them were reproducibly detected. Among those reproducibly detected, 12 metabolites were also found in EM extracts (Figure 3A). We focused our MS-based dereplication on these 12

https://doi.org/10.1021/acsomega.2c05415
ACS Omega 2022, 7, 43068−43083

Table 2. ^{1}H and ^{13}C NMR Data for A8 Acquired in CD_3OD (600 MHz) at 300 K

position	δ_C, type	measured δ_H (*J*, Hz)	[a]calculated δ_H (*J*, Hz)	HMBC
1	75.6, CH	4.07, d (0.9)	4.07, d (0.91)	2, 3, 5, 6, 7
2	114.3, C			
3	149.5, C			
4	123.0, C			
5	132.4, CH	6.42, d (0.9)	6.415, d (0.91)	1, 2, 3, 4, 6, 7
6	92.5, C			
7a	40.3, CH_2	3.78, d (18.2)	3.78, d (-18.16)	1, 5, 6, 8
7b		3.09, d (18.2)	3.09, d (-18.16)	
8	155.4, C			
9	161.9, CO			
10	39.7, CH_2	3.33, p dd (6.5, 2.3)	3.34, ddd (-13.41, 6.90, 6.29) 3.32, ddd (-13.41, 8.40, 5.90)	9, 11, 12
11	27.5, CH_2	1.64, m	1.640, ddddd (-12.40, 8.72, 8.40, 6.90, 6.75) 1.638, ddddd (-12.40, 7.74, 6.29, 5.90, 4.09)	10, 12, 13
12	26.4, CH_2	1.67, m	1.674, ddddd (-12.89, 9.46, 7.74, 6.75, 4.50) 1.668, ddddd (-12.89, 9.66, 8.72, 6.14, 4.09)	10, 11, 13
13	40.6, CH_2	2.93, p t (7.3)	2.94, ddd (-14.00, 9.66, 4.50) 2.93, ddd (-14.00, 9.46, 6.14)	11, 12
3-OMe	60.5, CH_3	3.73, s	3.73, s	3

[a]Calculated coupling constants by quantum mechanical analysis through ^{1}H iterative full spin analysis, using Cosmic Truth (https://ctb.nmrsolutions.fi/).[66,67] *p* = pseudo.

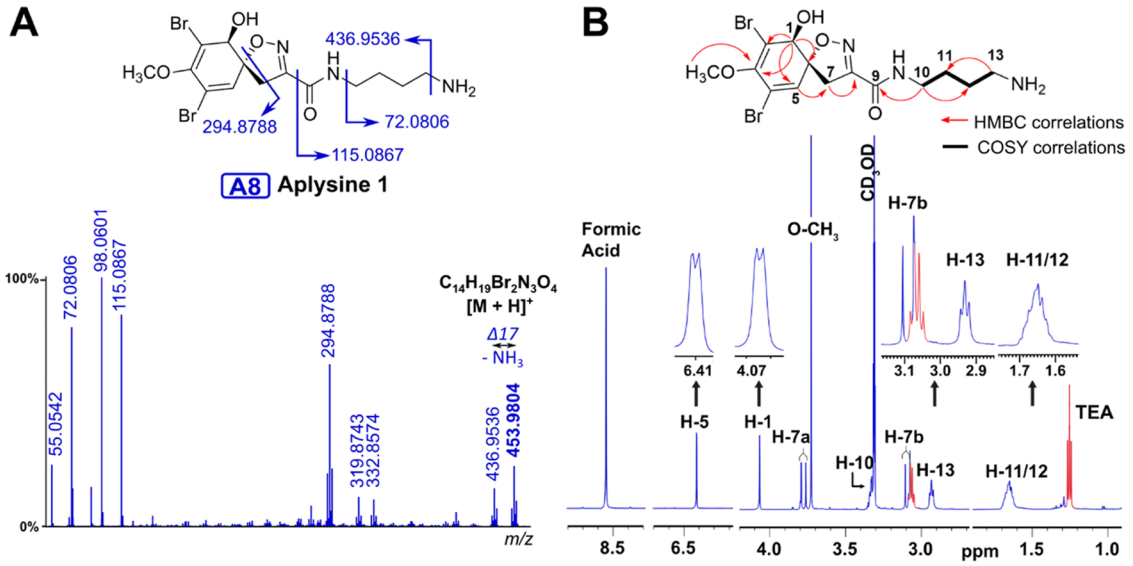

Figure 4. (A) Annotated MS^2 spectra of aplysine 1 (**A8**). This spectrum was generated using the GNPS Metabolomics USI interface and corresponds to a consensus spectrum. (B) Principal HMBC and COSY correlations observed for the structural assignment of aplysine 1 (**A8**). ^{1}H NMR spectra acquired in CD_3OD at 600 MHz. The ^{1}H NMR signals highlighted in red correspond to the triethylamine (TEA) buffer and formic acid used during purification.

molecules codified **A1** to **A12** (Table 1). Three of them (nodes **A5**, **A7** and **A9**) were found as single nodes in the molecular network; their molecular formulas were calculated based on their MS^1 data. One brominated metabolite, codified **B1**, and its isomer were reproducibly detected in EM extracts only. They were found in the third spectral family along with **A11**.

The first spectral family contained initially 89 nodes/chemical features (Figure 3B), corresponding to 61 molecules, including seven reproducibly detected in the EM extracts (Figure 3C). Their MS^2 spectra harbor a characteristic fragment at *m/z* 294.8786 $[C_8H_6Br_2O_2 + H]^+$, which has been described as a possible rearrangement of the dibromo-dihydroxy-methoxy-cyclohexadiene (Table 1).[52] This cluster of nodes encompasses the characteristic bromotyrosine spiroisoxazoline alkaloids. MS^2 dereplication enabled further annotation of brominated EMs by analytical propagation from node to node and comparison of data with those already published whenever possible (Figure 3C). The identity of aerothionin **A3** was further confirmed with the publicly shared MS^2 data on GNPS.[57] Compound **A1** was annotated as aerophobin 1 (M477T9.91 $[C_{15}H_{16}Br_2N_4O_4 + H]^+$)[58,59] and **A4** was annotated as purealidin L (M496T11.75 $[C_{15}H_{21}Br_2N_5O_4 + H]^+$).[52] Connected to purealidin L with a cosine score of 0.9, **A10** was attributed to aplysinamisine II (M510T13.19 $[C_{16}H_{23}Br_2N_5O_4 + H]^+$).[52,60] The annotated MS spectra are available in the Supporting Information. The compound **A8** ($[C_{14}H_{19}Br_2N_3O_4 + H]^+$) was found to be closely related to both **A3** and **A4** (cosine scores 0.74 and 0.80, respectively). Both its molecular formula and exact mass could match the structure as found in PubChem (CID: 101765254), *N*-(4 aminobutyl)-2-[(*E*)-hydroxyimino]-3-(2-hydroxy-3,5-dibromo-4-methoxyphenyl) propenamide but has not been reported to be isolated from any natural source.

https://doi.org/10.1021/acsomega.2c05415
ACS Omega 2022, 7, 43068−43083

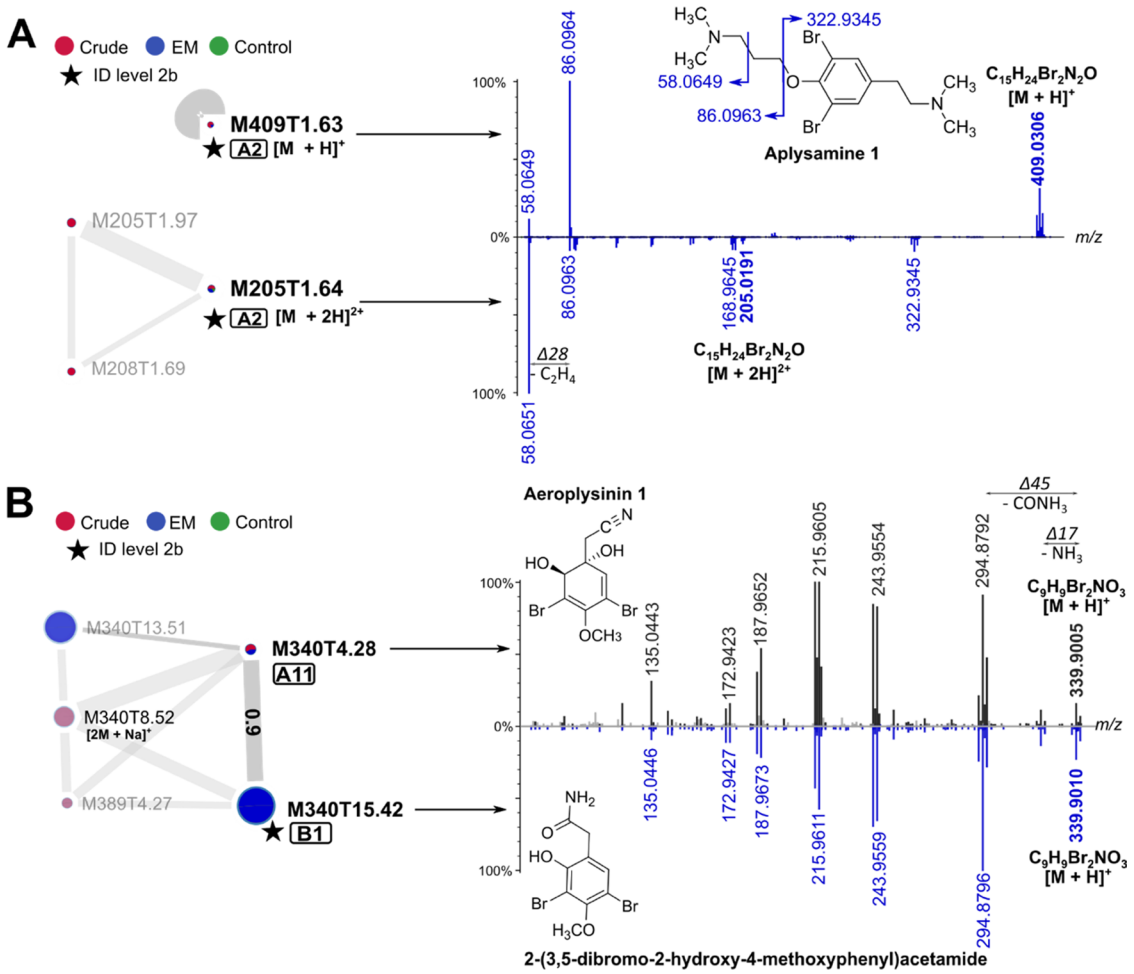

Figure 5. (A) Focus on spectral family 2 of **A2** identified as aplysamine-1. The MS^2 spectra in mirror match represent the fragmentation of **A2** $[M + H]^+$ (single node) compared to its $[M + 2H]^{2+}$. (B) Focus on identified metabolites within the spectral family of aeroplysinin-1 and isomers. The identity of **A11** detected in both crude and EM extracts was confirmed to be aeroplysinin-1 by comparison with a commercial standard, where MS^2 spectrum was deposited in the GNPS library (CCMSLIB00010012977). The isomer **B1**, only detected as EM, was annotated as 3,5-dibromo-2-hydroxy-4-methoxyphenylacetamide (confidence level of identification 2B).[62]

The MS^2 spectrum of **A8** revealed, in addition to the fragment at m/z 294.8786, one major fragment at m/z 115.0865 $[C_5H_{11}N_2O + H]^+$ followed by m/z 98.0601 $[C_5H_7NO + H]^+$, m/z 72.0805 $[C_4H_9N + H]^+$, and finishing with m/z 55.0540 $[C_4H_6 + H]^+$; all of those MS fragments together with the neutral loss of Δ17.0269 (NH_3) indicated the presence of an amide function connected to a C_4H_8 side chain and possibly substituted by a primary amine (NH_2)[52] (Figure 4). We further proceeded with the purification of **A8** from the sponge crude extract to confirm its identity by NMR (one-dimensional (1D) $^1H/^{13}C$ and two-dimensional (2D) gCOSY, HSQC, and HMBC). This compound was isolated after two steps of Vacuum Liquid Chromatography (VLC) fractionation followed by purification by preparative high-performance liquid chromatography (HPLC) (Figure S5), along with other abundant bromo-spiroisoxazolines, notably, **A1**, **A4**, and **A10**. The structural identity of such bromotyrosine spiroisoxazolines was confirmed by comparing their NMR data with those already published.[34,37,58−61]

Both ^1H and ^{13}C NMR spectra of **A8** showed characteristic chemical shifts of an ortho methoxy bromo-cyclohexadiene spiroisoxazoline, also observed for all isolated congeneric spiroisoxazolines (Table 2 and Figure 4). Briefly, two doublets characterized by a small coupling constant (J = 0.9 Hz), often described as singlets in the literature, were observed in the ^1H NMR spectrum at δ_H 6.42 (1H, H-5, d, $J_{H5\text{-}H1}$ = 0.9 Hz) and δ_H 4.07 (1H, H-1, d, $J_{H5\text{-}H1}$ = 0.9 Hz). A singlet corresponding to a methoxy group is present at δ_H 3.73. Finally, the protons at 3.78 (1H, H-7a, d, J = 18.2 Hz) and δ_H 3.09 (1H, H-7b, d, J = 18.2 Hz) were concluded to be diastereotopic methylene protons as both show HSQC correlations to C-7 (δ_C 40.3). Both gave correlation cross-peaks notably with C-1 and C-5 in the HMBC spectrum. Altogether, these five ^1H chemical shifts can serve as an NMR fingerprint of the bromotyrosine spiroisoxazoline alkaloids widely distributed in Verongiida sponges. Therefore, **A8** did not correspond to the structure with a PubChem CID of 101765254. The relative position of CH_2-10 to CH_2-13, was confirmed by HSQC and HMBC analyses. Likewise, the methylene CH_2-13 (δ_H 2.93, 2H, pt, δ_C 40.6) also showed HMBC correlations to C-11/12, thereby confirming its position at the end of the aliphatic chain made of four methylene units (Table 2 and Figures 4 and S7). The IR spectrum of **A8** (Supporting Information S10) confirmed the presence of a primary amine as an ammonium salt (~3269 cm^{-1}) together with aliphatic methylene (strong bands at 2959−2918 cm^{-1}).

https://doi.org/10.1021/acsomega.2c05415
ACS Omega 2022, 7, 43068−43083

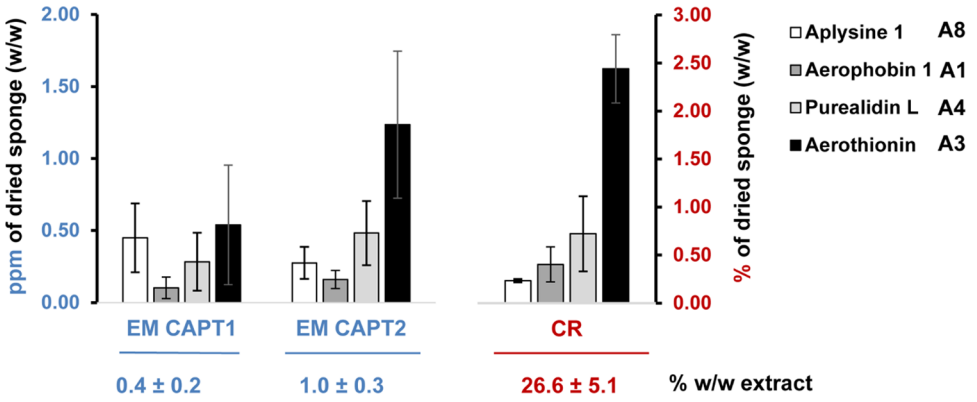

Figure 6. Concentration of the four most abundant bromo-spiroisoxazolines in the EM extracts for each set of reproduced experiments (n = 3 for CAPT1 and CAPT2) compared to their concentration in the sponge crude extract. The results are expressed as the proportion of weight/weight (w/w) in ppm and in percentage of dried sponge biomass for EM and crude, respectively. The quantities of all four metabolites in their respective extract are expressed in % w/w, below each bar graph.

Further quantum mechanical analyses were performed to precisely describe the absolute configuration of **A8**. First, comparative analysis of calculated ultraviolet/electronic circular dichroism (UV/ECD) spectra with the experimental one led to the conclusion that the absolute configuration of **A8** could be either (1*S*, 6*S*) or (1*R*, 6*S*) (Supporting Information S8). While the former configuration has never been reported for such class of alkaloids, the latter one agrees with the vast majority of described configurations for the spiroisoxazoline ring.[63,64] To further discriminate between the two possible diastereomers, quantum mechanical analyses of ^{13}C NMR chemical shifts by GIAO NMR and DP4+ calculations[65] were performed and led us to assign the relative configuration of **A8** to be *R/S* (Supporting Information S9). Therefore, combining the results from ECD and DP4+ calculations, we were able to unambiguously determine the absolute 1*R*, 6*S* configuration of **A8**. Lastly, multiplicity and complex splitting patterns observed in the ^{1}H NMR spectrum of **A8** were further determined by quantum mechanical analysis through ^{1}H iterative full spin analysis (Table 2),[66,67] using Cosmic Truth (https://ctb.nmrsolutions.fi/) to calculate the underlying coupling constants. Herein, described for the first time, the bromotyrosine spiroisoxazoline compound **A8** is named aplysine 1.

Building on this structural knowledge acquired for **A8**, the compounds **A6** and **A12** directly connected to **A8** could be further annotated by propagation (Figure 3C). The MS^2 spectrum of compound **A12** (M468T11.13 $[C_{15}H_{21}Br_2N_3O_4 + H]^+$) is highly similar to **A8** (cosine score: 0.93), and both its precursor ion $[M + H]^+$ and MS fragments differ by Δ14.0145, corresponding to the addition of one methylene unit to **A8**. The molecular formula and exact mass of **A12** could correspond to the compound (2*E*)-*N*-(5-aminopentyl)-3-(3,5-dibromo-2-hydroxy-4-methoxyphenyl)-2-hydroxyiminopropanamide as reported in PubChem (CID 11397182). The MS^2 spectrum of **A12** revealed, in addition to the fragment at m/z 294.8786, one major fragment at m/z 86.0963 $[C_5H_{11}N + H]^+$ and a second one at m/z 69.0696 $[C_5H_8 + H]^+$ with a neutral loss of Δ17.0269 (NH_3) in a similar manner than **A8**. Based on the structural knowledge acquired for **A8**, compound **A12** was annotated as a bromo-spiroisoxazoline derivative of **A8** harboring an additional methylene on the aliphatic chain. Compound **A6**, M496T12.05 (monoisotopic m/z 494.0283 $[C_{17}H_{25}Br_2N_3O_4 + H]^+$), was found to be closely related to **A12** (cosine score of 0.81). In addition to the characteristic fragments of the spiroisoxazoline moiety, the MS^2 spectrum of **A6** reveals two major fragments: one at m/z 157.1336 for $[C_8H_{16}N_2O + H]^+$ and the other at m/z 114.1277 corresponding to $[C_7H_{15}N + H]^+$. These MS^2 fragments suggested a structure similar to **A12** but harboring an aliphatic chain containing two additional methylene (Δ 28.0317) on the aliphatic amino side chain. Both **A6** and **A12** were present in trace amounts and could not be purified from the sponge crude extract in reasonable quantities to further confirm their structural identity by NMR. Following our MS-based analyses, and according to Schymanski et al.,[62] the confidence levels of identification for **A6** and **A12**, methylene congeners of **A8**, were set at level 2b.

The second spectral family of interest includes **A2**, M205T1.64 (m/z 204.0203 calculated for $[C_{15}H_{24}Br_2N_2O + 2H]^{2+}$), connected to three other nodes corresponding to metabolites only detected in the sponge biomass (Figure 5A). The molecular formula matches with the compound aplysinamine 1 (PubChem CID 362025) previously isolated from sponge species of the Verongiida order.[37,40] Further observation of its MS^2 spectrum revealed a fragment at m/z 322.9341 (monoisotopic m/z 320.9357 $[C_{10}H_{12}Br_2NO + H]^+$) corresponding to aplysamine-1 without its *N*-dimethylpropylamine side chain, one abundant fragment at m/z 58.0651 $[C_3H_7N + H]^+$ corresponding to the trimethylamine ion, and a smaller fragment at m/z 86.0963 $[C_5H_{11}N + H]^+$ confirming the presence of *N*-dimethylpropylamine, as previously described,[68] and in agreement with the proposed structure. Using the CFM-ID spectra prediction module, we also obtained a predicted MS^2 spectrum similar to the acquired one at 40 eV.[69] Accordingly, **A2** was annotated aplysinamine 1 in this study with a level 2b of confidence.[62]

The third brominated spectral family (Figure 5B) includes the MS^2 spectra of **A11** (M340T4.66, monoisotopic m/z 337.9022 $[C_9H_9Br_2NO_3 + H]^+$), whose calculated exact mass and molecular formula match aeroplysinin-1. Analysis of the MS^2 fragmentation pattern using MetFrag and interrogating several databases (*e.g.*, COCONUT,[70] ChEBI[71]) also suggested aeroplysinin-1 for **A11**, along with two other isomers: 3,5-dibromo-L-tyrosine and 3,5-dibromo-2-hydroxy-4-methoxyphenylacetamide. Both of them were already recorded in other Verongiida sponges.[72−76] Hence, aeroplysinin-1 and 3,5-dibromo-L-tyrosine were purchased to determine their MS^2 spectra and retention time under our analytical conditions. The MS^2 spectrum of purchased 3,5-dibromo-L-tyrosine did not

https://doi.org/10.1021/acsomega.2c05415
ACS Omega 2022, 7, 43068−43083

match those recorded within the spectral family. On the other hand, both the retention time and MS^2 spectrum of the commercial aeroplysinin-1 matched those of **A11**, whose structural identity was therefore confirmed. Uniquely present in the sponge EM, the closely related structure **B1** (M340T15.80: monoisotopic m/z 337.9017 $[C_9H_9Br_2NO_3 + H]^+$) has the same molecular formula and a nearly identical MS^2-fragmentation pattern than **A11**. The log *P* of 3,5-dibromo-2-hydroxy-4-methoxyphenylacetamide (log *P*: 2.2 at 25 °C, ACD/Labs) suggested a higher hydrophobicity with a higher retention time than aeroplysinin-1 **A11** (log *P* 1.0 at 25 °C, ACD/Labs). Moreover, the MS^2 spectrum of such an isomer was expected to share nearly identical fragment ions compared to those observed for **A11**, in particular, at m/z 292.8824 corresponding to the neutral loss Δ 45.0193 ($CONH_3$, loss of acetamide moiety) from the parent ion. Accordingly, the identity of **B1** (RT 15.8 min) was putatively attributed to 3,5-dibromo-2-hydroxy-4-methoxyphenylacetamide (CAS: 28495-12-7). This metabolite could be a "degradation" product of aeroplysinin-1 through nitrile hydration as previously reported.[39] Metabolite **B1** has also been detected in several Verongiida sponges such as *Aplysina thiona*,[75] *A. aerophoba*,[76] *Psammoposilla purpurea*,[73] and *Suberea mollis*,[74] supporting the proposed annotation with a level 2b of confidence.[62]

Quantification of the Most Abundant Bromo-Spiroisoxazoline Exometabolites. Our last objective was to determine the concentration of the most abundant reproducibly detected EMs in the enriched seawater extract compared to their respective concentration within the sponge biomass. The most abundant and reproducibly detected EMs are **A1, A3, A4**, and **A8.** Quantitative analysis, using calibration curves generated with purified metabolites, was performed on all of the EM replicates for CAPT1 and CAPT2 and on the sponge crude extract (Figures 6 and S13). Calculated quantification results were corrected by the purity of each metabolite determined by qHNMR.[77] The proportion between metabolites within the EM extracts remained constant but was found to differ from that in the crude extract. Hence, the composition of the four metabolites in EM extracts differed from their composition in the sponge crude extract. Aerothionin **A3** remained the most abundant metabolite both in EM and crude extracts. The sum of all four quantified exometabolites represented between 0.4 and 1.0% w/w of the recovered seawater extract.

As expected, those metabolites were found to be ∼25 times more concentrated in the sponge crude extract than they were in the concentrated seawater extract. Nevertheless, such seawater extract was collected around the sponge without touching its biomass or affecting its viability. Overall, the quantitative results, presented herein, are essential to help further optimizing the techniques for concentrating sponge EMs more efficiently. Repetitive or continuous EM captures/concentrations over time, on more sponge specimens, with the addition of external stimulations (*e.g.*, touching/milking),[25] are expected to lead to higher levels of specialized metabolites in the recovered seawater extract.

CONCLUSIONS

This study has demonstrated that the chemical composition of the exometabolome from *A. cavernicola* comprises brominated specialized metabolites, representing altogether 12% of the seawater recovered chemical signals. Those signals corresponded to a total of 13 bromotyrosine alkaloids reproducibly detected as EM, including one brominated alkaloid structurally related to aeroplysinin-1 and uniquely found in seawater. Aerothionin, purealidin L, aerophobin 1, and the newly described aplysine 1 were found to be the most abundant EMs. Hence, using a passive method of adsorption on XAD resins, we were able to reproducibly access 15% of the sponge-specialized metabolites, four of them accounting for 1.0% w/w of the total collected seawater extract. The data collected herein will guide future *in situ* field works and the development of sustainable methods focusing on concentrating specialized metabolites released not only by *A. cavernicola* but also by other marine species within their ecosystem. We herein observed that the proportion of the four most abundant metabolites in seawater around the sponge differs from the one measured in the sponge biomass. Such results will contribute to design experiments aiming to evaluate whether those specialized brominated EMs play a role in marine chemical mediation and the functioning of ecosystems. With a total of 127 brominated alkaloids detected in the set of crude extracts, our metabolomic analyses also highlighted the large reservoir of potentially new bromotyrosine spiroisoxazoline derivatives yet to be described from *A. cavernicola*. The present work underlines the potential of sponge's exometabolomes as a source of molecules that could be collected from seawater, enriched, and later be screened for their biological properties with minimal to no impact on marine biodiversity.

EXPERIMENTAL SECTION

General Experimental Procedures. All UHPLC-MS-grade solvents (methanol [MeOH], acetonitrile [MeCN], and water) were purchased from Carlo Erba. The Amberlite XAD resins XAD-7 (Alfa Aesar), as well as the C-18 silica powder (Polygoprep 60-50, Macherey-Nagel) were purchased from VWR (VWR International, LLC). C18 SPE cartridges (Strata C18-E, 70 Å, 500 mg/6 mL) were purchased from Phenomenex. The commercial standards 3,5-dibromo-L-tyrosine (CAS: 300-38-9, MW 338.98 g/mol, molecular formula $C_8H_9Br_2NO_3$) and (+) aeroplysinin-1 (CAS: 28656-91-9, *M*W 338.98 g/mol, molecular formula $C_9H_9Br_2NO_3$) were purchased from Toronto Research Chemicals and Cayman Chemical Company, respectively. UHPLC-MS analyses were performed on a Luna Omega Polar C18, 1.6 μm 100 Å column (150 mm × 2.1 mm, Phenomenex) using a Thermo Scientific Dionex Ultimate 3000 UHPLC system equipped with a diode array detector and connected to an electrospray-ionisation-quadrupole time-of-flight (ESI-Q-TOF) IMPACT II mass spectrometer (software Bruker Otof Control version 4.1). LC-MS data processing was performed on the Compass DataAnalysis software (Bruker Version 5.0) and with Mzmine 2 (version 2.53). Preparative HPLC was performed on a GILSON PLC 2020 instrument (Gilson Inc.) using a Luna Omega Polar C18 column 5 μm (250 mm × 21.2 mm, Phenomenex). NMR analyses were performed on a Bruker Avance II+ spectrometer at 600 MHz equipped with a TCI Cryoprobe at 300 K. The acquired spectra were processed using Topspin 4.1.1 NMR software package (Bruker BioSpin). Iterative full spin analyses were performed with the β version of Cosmic Truth (CT) (https://ctb.nmrsolutions.fi). ECD spectra were measured on a JASCO J-815 spectropolarimeter equipped with a JASCO Peltier cell holder PTC-423 at 20 °C in quartz cells of 1 mm path length. Fourier-transform infrared spectroscopy (FTIR) spectra were collected on a Bruker VERTEX70 FTIR spectrometer equipped with a Bruker A222 attenuated

https://doi.org/10.1021/acsomega.2c05415
ACS Omega 2022, 7, 43068−43083

total reflection (ATR) from pure samples deposited on diamond crystals at 25 °C.

Sponge Collection and Identification. Samples of *A. cavernicola* were collected, fixed on their rocky substrate by Scuba diving in the bay of Marseille, at the entrance of the submarine cave (43°12′634 N/5°19′968 E), where this species is dominant, in November 2020 and May 2021. These samples were collected in agreement with the Nagoya Protocol with the French National Declaration under the receipt TREL2022990S I 392 and the Internationally Recognized Certificate of Compliance (IRCC) Number ABSCH-IRCC-FR-253848-1 available to the Access and Benefit-sharing Clearing-House (https://absch.cbd.int/about/). All collected sponge specimens were transported in hermetic jars of seawater without exposure to air. Upon arrival at the laboratory, sponges (∼100 cm^3) were transferred in 50 L aquaria with constant renewal of filtered seawater maintained at 16 °C. Specimens were inspected after the 24-h acclimation period and before starting each experiment to assess their health status (maintenance of the biomass yellow coloration, opening of oscula) and check the absence of possible epibiosis, white bacterial veil, or dark spots of tissue necrosis. Animals were not manipulated or touched during the entire duration of the experiments in aquaria.

Continuous Adsorption of Exometabolites. For each aquarium (50 L), the adsorption of dissolved and diluted metabolites on polymeric XAD-7 resin was performed over a 16-h period in a closed water circuit. The seawater temperature was maintained at 16 °C. The resin XAD-7 (50 g) was filled in a cartridge connected to an immersible pump (flow rate 5500 L/h, NewJet NJ 600). After each 16-h adsorption, the water was completely renewed in the aquarium for at least 8 h. Sponge health was checked during the entire course of the experiment as described above. In parallel, to adsorb seawater metabolites that will serve as analytical control, the same setup was performed in another 50 L aquarium without any sponges but filled with the same seawater. Each cycle of adsorption experiment was repeated three times for each sponge sample collected in November 2020 (CAPT1) and May 2021 (CAPT2). After each cycle of adsorption, the collected XAD-7 resin was washed with three bed volumes of ultrapure water to remove sea salts. The resin was eluted with three bed volumes of MeOH and one bed volume of 50% MeOH in water to recover all adsorbed metabolites. Extracts obtained from the elution of XAD-7 resins associated with the aquarium containing sponges were called exo-metabolite (EM) extracts, whereas extracts obtained from the elution of XAD-7 in the aquarium without sponges were identified as controls. Both EM extracts and controls were further desalted by solid-phase extraction (SPE) on Strata C18-E cartridges following the same protocol described for the sponge crude extract. The final weights of each recovered extract were as follows for CAPT1: EM1 20.1 mg, EM2 12.1 mg, EM3 18.2 mg, control1 7.2 mg, control2 5.8 mg, and control3 4.4 mg. For CAPT2, the final recovered extract weights were EM1 10.5 mg, EM2 6.1 mg, EM3 12.4 mg, control1 6.2 mg, control2 3.9 mg, and control3 4.4 mg. All samples were diluted in an MS-grade solvent and prepared at 0.5 mg/mL.

Preparation of Sponge Crude Extracts. At the end of the capture experiments, *A. cavernicola* sponges were flash frozen in liquid nitrogen, stored at -80 °C, and then freeze-dried for 48-h (Heto PowerDry PL3000 Freeze Dryer, Thermo). The dried sponge biomass was reduced to a thin powder with a knife mill (M20, IKA-WERKE) yielding 42.4 g for CAPT1 and 46.0 g for CAPT2. Approximately one gram of sponge powder was mixed with 10 mL of MeOH LC-grade, sonicated for 5 min (J.P SELECTA, 50/60 Hz), followed by a 30 min maceration at room temperature. The mixture was filtered under vacuum, and the remaining sponge powder was rinsed with 10 mL of MeOH. Crude extracts adsorbed on 100 mg of C18 powder (Polygoprep 60-50, MN) were further processed on Strata C18-E SPE cartridges to remove residual sea salts. Extracts were washed with 18 mL of LC-MS-grade water and then eluted with 12 mL of MS-grade MeOH, thereby leading to the production of desalted *A. cavernicola* crude extracts, with a calculated extraction yield of 13.6% w/w (weight extract/weight dried sponge biomass) for CAPT1 and 14.8% w/w for CAPT2. Crude extracts were prepared at 0.5 mg/mL in MS-grade MeOH.

UHPLC-UV HR-MS Acquisitions. All samples prepared in 100% of MS-grade MeOH were filtered on PTFE luer-lock filters (0.22 μm, cat#26142, Restek) prior to injection. Chromatographic separations were achieved on a Luna Omega Polar C-18 UHPLC column, maintained at 42 °C, with an elution gradient composed of (A) water and (B) MeCN both with 0.1% formic acid, under the following conditions: from 10% (B) during 2 min to 32.5% (B) at 15 min, then to 70% (B) at 17 min, and during 3 min (flow rate 0.45 mL/min, injection volume 2 μL). Mass spectrometry detection (Bruker Impact II qTOF) parameters in ESI positive mode were set as follows: nebulizer gas N_2 at 3.5 bars; dry gas at 12 L/min, capillary temperature at 200 °C, and voltage at 4500 V. MS/MS acquisition mode was set with a scan rate of 4 Hz (full scan 50−1200 m/z) and a mixed collision energy 20−40 eV (50% time at each collision energy, stepping mode). A sodium formate/acetate solution forming clusters on the studied mass range was used as calibrant and automatically injected before each sample for internal mass calibration, ensuring a precision of m/z lower than 2 ppm on the mass range. Extracts were randomly injected to integrate any memory effect on the column and time-dependent MS drift. Pooled samples, injected every six samples from the beginning to the end of the series, were used for further ion filtering.

UHPLC-MS Data Processing. Following their calibration, the acquired MS data were converted to the open format *.mzXML and further processed on MZmine 2.53[55] for feature detection as follows: (1) mass detection (centroid, MS^1, noise level 1E3, and MS^2 noise level 1E2), (2) ADAP chromatogram builder[78] (two scans, group intensity threshold 3E2, minimum highest intensity 3E2, m/z tolerance 10 ppm), (3) chromatogram deconvolution (algorithm baseline cut-off: minimum peak height 2E3, peak duration range 0.01−2.00 min, baseline level 1E3, range for MS^2 scan pairing 0.02 Da, and RT range for MS^2 scan pairing 0.03 min), (4) isotope peak grouper (m/z tolerance 10 ppm, RT tolerance 0.2 min, monotonic shape, representative isotope: most intense), (5) join aligner (m/z tolerance 10 ppm, weight for m/z 75%, RT tolerance 0.2 min, weight for RT 25%), and (6) feature list rows filter (RT 1.00−20.00 min and keeping only peaks with MS^2 scans). Features detected only in MeOH were deleted. The MS1 aligned feature list contained 2508 detected signals, and the MS^2 feature list contained 2411 signals.

Multivariate Data Analysis. The MS1 feature list exported as .csv file was processed on the MetaboAnalyst 5.0 web application (https://www.metaboanalyst.ca/home.xhtml) as follows: data integrity check was set as default, log-transformed, and normalized by Pareto scaling. The selection of main chemical features related to brominated metabolites between the three groups (EM, crude, and control) was achieved by selecting the first 30 variable importance in projection (VIP) for

https://doi.org/10.1021/acsomega.2c05415
ACS Omega 2022, 7, 43068−43083

component 1 (19.9% of variance) of the Partial Least-Square Discriminant Analysis (PLS-DA) plots. A permutation test (999 permutations, PPLSDA models) based on a double cross-validation followed by pairwise post-hoc permutational test was performed for the differentiation of each group of chemical fingerprints. The classification error rate (CER, 0−1) was calculated to estimate the strength of the generated models, using R software (version 4.1.0.) with the RVAideMemoire (version 0.9-80) package.

Feature-Based Molecular Networking. The feature quantification table and the corresponding list of MS^2 spectra linked to the MS^1 features (.mgf file format) were exported from MZmine 2.53 for feature-based molecular networking on the GNPS platform (https://gnps.ucsd.edu).[43] The precursor ion mass tolerance was set to 0.02 Da and the MS/MS fragment ion tolerance was set to 0.02 Da. A molecular network was then created where edges were filtered to have a cosine score above 0.7 and more than six matched peaks between MS^2 spectra. Further, edges between two nodes were only kept in the network if each of the nodes appeared in each other's respective top 10 most similar nodes. Finally, the maximal size of a molecular family was set at 100, and the lowest scoring edges were removed from molecular families until the molecular family size was below this threshold. The acquired MS^2 spectra in the network were then searched against GNPS spectral libraries.[57] The resulting network was visualized and interpreted using Cytoscape 3.8.[56]

Computational Analysis of Exometabolite Molecular Diversity. A total of 83 non-brominated chemical signals detected in all exometabolite (EM) extracts from CAPT1 and CAPT2 were analyzed in SIRIUS computational annotation tools (version 4.9.9).[28] De novo molecular formulas were computed with SIRIUS by matching the experimental and predicted isotopic patterns and following analysis of the fragmentation trees. Parameters were set as follows: molecular formula candidates retained = 10, profile (Q-TOF), m/z maximum deviation = 10 ppm, all adducts were considered, Sirius score threshold = 100, and all databases and fallback adducts were selected for CSI/FingerID structure elucidation. CANOPUS module was also selected enabling the assignment of exometabolites in different structural classes.[53] A total of 42 exometabolite features were excluded from the analysis due to noisy MS^2 fragmentation spectra.

Purification and Identification of Bromotyrosine Metabolites. *A. cavernicola* crude extract (6.14 g) was partitioned on C18 polygoprep (45 g) by vacuum liquid chromatography (VLC) with a 25% elution gradient ranging from 100% water to 100% MeOH and finally to 100% dichloromethane thereby leading to nine fractions of 100 mL each. Fraction 2 (169 mg, 25% MeOH in water) and fraction 3 (230 mg, 50% MeOH in water) were further submitted to preparative chromatography using a Luna Omega Polar C18 5 μm 100 Å (250 mm × 21.2 mm). The chromatographic elution was performed with ultrapure water (A) and HPLC-grade MeCN (B) both buffered with 0.1% v/v formic acid and 10 mM triethylamine (HiPerSolv Chromanorm, VWR chemicals) with the following gradient: from 15% B during 2.5 min up to 30% in 30 min. The applied flow rate was 20 mL/min, and 350−500 μL of fractions at ∼50 mg/mL were injected each time. Aplysine 1 (1 mg) eluted at 19 min, closely followed by aerophobin 1 (0.9 mg), purealidin J (1.4 mg) at 22.5 min, purealidin L (4.2 mg) at 24 min, aerophobin 2 (3.8 mg) at 25.5 min, and aplysinamisine I (2.5 mg) at 27 min (Figure S5). Likewise, aerothionin (4.1 mg) was purified by preparative HPLC from VLC fraction four. The identity of each purified bromo-spiroisoxazoline alkaloid derivative was confirmed by corroborating NMR (1D, 2D) and MS^2 data to previously published studies.[34,37,58−61] The structural characterization of aplysine 1 was performed by 1D NMR (^{1}H, ^{13}C) as well as 2D NMR analyses using nonuniform sampling pulses (2D gCOSY, gHSQC, and gHMBC) under quantitative conditions on a Bruker Avance II+ 600 MHz equipped with TCI Cryoprobe. Aplysine 1 (1 mg) was exactly weighed and diluted in 85 μL of deuterated MeOH (CD_3OD 99.96%-d, Eurisotop Cambridge Isotope Laboratories, Inc. #D048T) and then transferred in 2 mm o.d. NMR tubes (Bruker # 67539). ^{1}H and ^{13}C chemical shifts (δ) were expressed in ppm with reference to the residual solvent signal.

Computational Analysis for the Determination of Aplysine 1 Absolute Configuration. For the calculation of the UV-ECD spectra, conformational analyses of aplysine 1 were performed using annealing as implemented in AMPAC11 and density functional theory (DFT) with Gaussian 16. The geometries of the retained conformations were optimized at the SMD(acetonitrile)/B3LYP/6-311G(d,p) level where SMD is an IEF-PCM implicit solvation model.[79] Average UV-ECD spectra were calculated by averaging spectra of each selected conformation, weighted by its Boltzmann population. Further experimental details with calculated UV-ECD spectra are available in Supporting Information S8. Quantum mechanical calculations of ^{13}C NMR chemical shift were computed using gauge-independent atomic orbital (GIAO) NMR in Gaussian 16 and DP4+ probability calculations to determine the best fit to the experimental data from the diastereomeric models, as previously described.[65] The GIAO shielding constants of the major conformers (Boltzmann weight more than 1%) of each isomer were computed at the B3LYP/6-31+G(d,p) level in methanol and then averaged based on Boltzmann distribution. Due to spin−orbit coupling effects, poor calculated results could be produced for Br-substituted carbons, so they were excluded from DP4+ analysis.[80] Further experimental details and DP4+ results are available in Supporting Information S9.

LC-MS Quantification of Bromo-spiroisoxazoline Exometabolites. A calibration solution was prepared with each isolated metabolite as follows: purealidin L (purity: 79% w/w) and aerothionin (purity: 85% w/w) were added to a mixture of aplysine 1 and aerophobin 1 (purity ratio 35/48% w/w) to constitute a stock solution of the four isolated compounds from which serial dilutions were prepared. The concentration of each isolated metabolite was corrected by its purity determined by quantitative ^{1}H NMR using the 100% method as previously described[77] (calculation spreadsheet available at https://gfp.people.uic.edu/qnmr/content/qnmrcalculations/index.html). The calibration solutions, as well as the EM and crude extracts, were analyzed in triplicate within the same sequence of analysis and using UHPLC-ESI-MS acquisition parameters and chromatographic elution as described above. Logarithmic calibration curves were established by measuring the area under the curves of extracted ions chromatogram (EIC) for each of the nine concentrations ranging from 0.024 mg/mL to 0.094 μg/mL for aplysine 1, from 0.033 mg/mL to 0.13 μg/mL for aerophobin 1, from 9.87 to 0.038 μg/mL for purealidin L, and from 0.12 mg/mL to 0.46 μg/mL for aerothionin (Figure S12). The limits of detection (LOD) and quantitation (LOQ) were determined at a signal-to-noise ratio superior or equal to 3 and 10, respectively.

https://doi.org/10.1021/acsomega.2c05415
ACS Omega 2022, 7, 43068−43083

Aplysine 1. White amorphous powder; ECD (c 0.22 mM, MeCN) λ_{max} ($\Delta\varepsilon$) 194 (-12.7), 241 (+8.17), 288 (+6.3) nm; UV (c 0.22 mM, MeCN) λ_{max} (log ε) 194 (4.46), 220 (4.24), and 292 (3.69); IR (ATR, diamond) ν_{max} 3269, 2959, 2918, 2851, 1674, 1647, 1458, 1364, 1323, 1161, 824, 743, 675 cm^{-1}; HR-MS (ESI-qTOF) m/z 451.9821 $[M + H]^+$ (calcd for $C_{14}H_{20}Br_2N_3O_4$, 451.9815), MS^2 fragments acquired at CE: 20−40 eV, see Table 1. ^1H and ^{13}C NMR data (in CD_3OD), see Table 2.

■ ASSOCIATED CONTENT

Supporting Information

The Supporting Information is available free of charge at https://pubs.acs.org/doi/10.1021/acsomega.2c05415.

Photos of *A. cavernicola* (S1); comparative adsorption capacities of XAD resins (S2); PLS-DA score plot (S3); feature-based molecular network of the entire Dataset (S4); preparative HPLC chromatogram of fraction 2 used for the purification of aplysine 1 (S5); annotated MS^2 spectra of identified bromotyrosine spiroisoxazolines (S6); assigned NMR spectra of aplysine 1 (S7); ECD analyses of aplysine 1 (S8); GIAO NMR and DP4+ analyses of aplysine 1 (S9); IR spectrum of aplysine 1 (S10); assigned ^1H NMR spectra and ^{13}C NMR data of isolated bromo-spiroisoxazoline alkaloids (S11 and S12); MS-based calibration curves used for the quantification of bromo-spiroisoxazoline EM (S13); raw MS^2 data (*mzxml) are freely available at the UCSD Center for Computational Mass Spectrometry database with the MassIVE identifier MSV000089502; all MS^2 spectra and NMR raw data of purified bromotyrosine spiroisoxazolines are made freely available at https://doi.org/10.5281/zenodo.4679500; molecular networking job can be accessed at https://gnps.ucsd.edu/ProteoSAFe/status.jsp?task=1e6e7a9600c84391b3e249e9527a7142 (PDF)

■ AUTHOR INFORMATION

Corresponding Author

Charlotte Simmler − *IMBE, UMR CNRS 7263, IRD 237, Aix Marseille Université, Avignon Université, Endoume Marine Station, 13007 Marseille, France;* orcid.org/0000-0002-6923-2630; Phone: +033 4.13.94.50.49; Email: charlotte.simmler@imbe.fr

Authors

Morgane Mauduit − *IMBE, UMR CNRS 7263, IRD 237, Aix Marseille Université, Avignon Université, Endoume Marine Station, 13007 Marseille, France;* orcid.org/0000-0003-4583-5389

Stéphane Greff − *IMBE, UMR CNRS 7263, IRD 237, Aix Marseille Université, Avignon Université, Endoume Marine Station, 13007 Marseille, France;* orcid.org/0000-0001-9156-5194

Gaëtan Herbette − *Aix Marseille Université, CNRS, Centrale Marseille, FSCM-Spectropole, 13397 Marseille, France;* orcid.org/0000-0002-3374-2508

Jean-Valère Naubron − *Aix Marseille Université, CNRS, Centrale Marseille, FSCM-Spectropole, 13397 Marseille, France;* orcid.org/0000-0002-8523-4476

Sara Chentouf − *Aix Marseille Université, CNRS, Centrale Marseille, FSCM-Spectropole, 13397 Marseille, France;* orcid.org/0000-0003-0695-7260

Trung Huy Ngo − *College of Pharmacy, Yeungnam University, Gyeongsan-si, Gyeongsangbuk-do 38541, South Korea*

Joo-Won Nam − *College of Pharmacy, Yeungnam University, Gyeongsan-si, Gyeongsangbuk-do 38541, South Korea;* orcid.org/0000-0001-5502-0736

Sacha Molinari − *IMBE, UMR CNRS 7263, IRD 237, Aix Marseille Université, Avignon Université, Endoume Marine Station, 13007 Marseille, France*

Fathi Mabrouki − *IMBE, UMR CNRS 7263, IRD 237, Aix Marseille Université, Avignon Université, Faculté de Pharmacie, 13385 Marseille, France*

Elnur Garayev − *IMBE, UMR CNRS 7263, IRD 237, Aix Marseille Université, Avignon Université, Faculté de Pharmacie, 13385 Marseille, France;* orcid.org/0000-0003-4790-4878

Béatrice Baghdikian − *IMBE, UMR CNRS 7263, IRD 237, Aix Marseille Université, Avignon Université, Faculté de Pharmacie, 13385 Marseille, France;* orcid.org/0000-0001-8930-338X

Thierry Pérez − *IMBE, UMR CNRS 7263, IRD 237, Aix Marseille Université, Avignon Université, Endoume Marine Station, 13007 Marseille, France*

Complete contact information is available at: https://pubs.acs.org/10.1021/acsomega.2c05415

Notes

The authors declare no competing financial interest.

■ ACKNOWLEDGMENTS

The authors acknowledge financial supports by the ANR (ANR-20-CE43-0003-01) and the CNRS fellowship for M. Mauduit's PhD. The authors are deeply grateful to the team of marine biologists: Drs. Jean Vacelet, Nicole Boury-Esnault, Christophe Lejeusne, Pierre Chevaldonné, and Alexander Ereskovsky for fruitful conversations, notably regarding Aplysina's biology, and other related topics. M.M., G.H. and C.S. are thankful to Dr. Oliver Bornet in charge of the NMR facility at the Marseille Institute of Microbiology (IMM, FR3479).

■ REFERENCES

(1) Pita, L.; Rix, L.; Slaby, B. M.; Franke, A.; Hentschel, U. The Sponge Holobiont in a Changing Ocean: From Microbes to Ecosystems. *Microbiome* **2018**, *6*, No. 46.

(2) Paul, V. J.; Puglisi, M. P. Chemical Mediation of Interactions among Marine Organisms. *Nat. Prod. Rep.* **2004**, *21*, 189−209.

(3) Pawlik, J.; Chanas, B.; Toonen, R.; Fenical, W. Defenses of Caribbean Sponges against Predatory Reef Fish. I. Chemical Deterrency. *Mar. Ecol.: Prog. Ser.* **1995**, *127*, 183−194.

(4) Thoms, C.; Ebel, R.; Proksch, P. Activated Chemical Defense in Aplysina Sponges Revisited. *J. Chem. Ecol.* **2006**, *32*, 97−123.

(5) Thoms, C.; Schupp, P. J. Chemical Defense Strategies in Sponges: A Review. *Porifera Res.: Biodiversity, Innovation Sustainability* **2007**, *28*, 627−637.

(6) Weiss, B.; Ebel, R.; Elbrächter, M.; Kirchner, M.; Proksch, P. Defense Metabolites from the Marine Sponge *Verongia aerophoba*. *Biochem. Syst. Ecol.* **1996**, *24*, 1−12.

(7) Gerwick, W. H.; Moore, B. S. Lessons from the Past and Charting the Future of Marine Natural Products Drug Discovery and Chemical Biology. *Chem. Biol.* **2012**, *19*, 85−98.

(8) Jimenez, P. C.; Wilke, D. V.; Branco, P. C.; Bauermeister, A.; Rezende-Teixeira, P.; Gaudêncio, S. P.; Costa-Lotufo, L. V. Enriching Cancer Pharmacology with Drugs of Marine Origin. *Br. J. Pharmacol.* **2020**, *177*, 3−27.

(9) Laport, M.; Santos, O.; Muricy, G. Marine Sponges: Potential Sources of New Antimicrobial Drugs. *Curr. Pharm. Biotechnol.* **2009**, *10*, 86−105.
(10) Mehbub, M.; Lei, J.; Franco, C.; Zhang, W. Marine Sponge Derived Natural Products between 2001 and 2010: Trends and Opportunities for Discovery of Bioactives. *Mar. Drugs* **2014**, *12*, 4539−4577.
(11) Carroll, A. R.; Copp, B. R.; Davis, R. A.; Keyzers, R. A.; Prinsep, M. R. Marine Natural Products. *Nat. Prod. Rep.* **2021**, *38*, 362−413.
(12) de Goeij, J. M.; van Oevelen, D.; Vermeij, M. J. A.; Osinga, R.; Middelburg, J. J.; de Goeij, A. F. P. M.; Admiraal, W. Surviving in a Marine Desert: The Sponge Loop Retains Resources Within Coral Reefs. *Science* **2013**, *342*, 108−110.
(13) McMurray, S. E.; Stubler, A. D.; Erwin, P. M.; Finelli, C. M.; Pawlik, J. R. A Test of the Sponge-Loop Hypothesis for Emergent Caribbean Reef Sponges. *Mar. Ecol.: Prog. Ser.* **2018**, *588*, 1−14.
(14) Wulff, J. Ecological Interactions and the Distribution, Abundance, and Diversity of Sponges. In *Advances in Sponge Science: Phylogeny, Systematics, Ecology*; Elsevier, 2012; Vol. *61*, pp 273−344.
(15) Topçu, N. E.; Pérez, T.; Grégori, G.; Harmelin-Vivien, M. *In Situ* Investigation of *Spongia officinalis* (Demospongiae) Particle Feeding: Coupling Flow Cytometry and Stable Isotope Analysis. *J. Exp. Mar. Biol. Ecol.* **2010**, *389*, 61−69.
(16) Santonja, M.; Greff, S.; Le Croller, M.; Thomas, O. P.; Pérez, T. Distance Interaction between Marine Cave-Dwelling Sponges and Crustaceans. *Mar. Biol.* **2018**, *165*, No. 121.
(17) Thompson, J. E. Exudation of Biologically-Active Metabolites in the Sponge *Aplysina fistularis* I. Biological Evidence. *Mar. Biol.* **1985**, *88*, 23−26.
(18) Nebbioso, A.; Piccolo, A. Molecular Characterization of Dissolved Organic Matter (DOM): A Critical Review. *Anal. Bioanal. Chem.* **2013**, *405*, 109−124.
(19) Catalá, T. S.; Shorte, S.; Dittmar, T. Marine Dissolved Organic Matter: A Vast and Unexplored Molecular Space. *Appl. Microbiol. Biotechnol.* **2021**, *105*, 7225−7239.
(20) Kelly, L. W.; Nelson, C. E.; Petras, D.; Koester, I.; Quinlan, Z. A.; Arts, M. G. I.; Nothias, L.-F.; Comstock, J.; White, B. M.; Hopmans, E. C.; van Duyl, F. C.; Carlson, C. A.; Aluwihare, L. I.; Dorrestein, P. C.; Haas, A. F. Distinguishing the Molecular Diversity, Nutrient Content, and Energetic Potential of Exometabolomes Produced by Macroalgae and Reef-Building Corals. *Proc. Natl. Acad. Sci.* **2022**, *119*, No. e2110283119.
(21) Petras, D.; Koester, I.; Da Silva, R.; Stephens, B. M.; Haas, A. F.; Nelson, C. E.; Kelly, L. W.; Aluwihare, L. I.; Dorrestein, P. C. High-Resolution Liquid Chromatography Tandem Mass Spectrometry Enables Large Scale Molecular Characterization of Dissolved Organic Matter. *Front. Mar. Sci.* **2017**, *4*, No. 405.
(22) Walker, R. P.; Thompson, J. E.; Faulkner, D. J. Exudation of Biologically-Active Metabolites in the Sponge *Aplysina fistularis* II. Chemical Evidence. *Mar. Biol.* **1985**, *88*, 27−32.
(23) Richelle-Maurer, E.; De Kluijver, M. J.; Feio, S.; Gaudêncio, S.; Gaspar, H.; Gomez, R.; Tavares, R.; Van de Vyver, G.; Van Soest, R. W. M. Localization and Ecological Significance of Oroidin and Sceptrin in the Caribbean Sponge *Agelas conifera*. *Biochem. Syst. Ecol.* **2003**, *31*, 1073−1091.
(24) Mehbub, M. F.; Tanner, J. E.; Barnett, S. J.; Franco, C. M. M.; Zhang, W. The Role of Sponge-Bacteria Interactions: The Sponge *Aplysilla rosea* Challenged by Its Associated Bacterium Streptomyces ACT-52A in a Controlled Aquarium System. *Appl. Microbiol. Biotechnol.* **2016**, *100*, 10609−10626.
(25) Ternon, E.; Zarate, L.; Chenesseau, S.; Croué, J.; Dumollard, R.; Suzuki, M. T.; Thomas, O. P. Spherulization as a Process for the Exudation of Chemical Cues by the Encrusting Sponge *C. Crambe*. *Sci. Rep.* **2016**, *6*, No. 29474.
(26) Vlachou, P.; Le Goff, G.; Alonso, C.; Álvarez, P.; Gallard, J.-F.; Fokialakis, N.; Ouazzani, J. Innovative Approach to Sustainable Marine Invertebrate Chemistry and a Scale-Up Technology for Open Marine Ecosystems. *Mar. Drugs* **2018**, *16*, No. 152.
(27) Hoffmann, M. A.; Nothias, L.-F.; Ludwig, M.; Fleischauer, M.; Gentry, E. C.; Witting, M.; Dorrestein, P. C.; Dührkop, K.; Böcker, S. High-Confidence Structural Annotation of Metabolites Absent from Spectral Libraries. *Nat. Biotechnol.* **2022**, *40*, 411−421.
(28) Dührkop, K.; Fleischauer, M.; Ludwig, M.; Aksenov, A. A.; Melnik, A. V.; Meusel, M.; Dorrestein, P. C.; Rousu, J.; Böcker, S. SIRIUS 4: A Rapid Tool for Turning Tandem Mass Spectra into Metabolite Structure Information. *Nat. Methods* **2019**, *16*, 299−302.
(29) Grenier, M.; Ruiz, C.; Fourt, M.; Santonja, M.; Dubois, M.; Klautau, M.; Vacelet, J.; Boury-Esnault, N.; Pérez, T. Sponge Inventory of the French Mediterranean Waters, with an Emphasis on Cave-Dwelling Species. *Zootaxa* **2018**, *4466*, No. 205.
(30) Reverter, M.; Perez, T.; Ereskovsky, A. V.; Banaigs, B. Secondary Metabolome Variability and Inducible Chemical Defenses in the Mediterranean Sponge *Aplysina cavernicola*. *J. Chem. Ecol.* **2016**, *42*, 60−70.
(31) Thoms, C.; Wolff, M.; Padmakumar, K.; Ebel, R.; Proksch, P. Chemical Defense of Mediterranean Sponges *Aplysina cavernicola* and *Aplysina aerophoba*. *Z. Naturforsch., C* **2004**, *59*, 113−122.
(32) Ciminiello, P.; Fattorusso, E.; Forino, M.; Magno, S.; Pansini, M. Chemistry of Verongida Sponges VIII - Bromocompounds from the Mediterranean Sponges *Aplysina aerophoba* and *Aplysina cavernicola*. *Tetrahedron* **1997**, *53*, 6565−6572.
(33) Kunze, K.; Niemann, H.; Ueberlein, S.; Schulze, R.; Ehrlich, H.; Brunner, E.; Proksch, P.; Pée, K.-H. Brominated Skeletal Components of the Marine Demosponges, *Aplysina cavernicola* and *Ianthella basta*: Analytical and Biochemical Investigations. *Mar. Drugs* **2013**, *11*, 1271−1287.
(34) Lira, N. S.; Montes, R. C.; Tavares, J. F.; da Silva, M. S.; da Cunha, E. V. L.; de Athayde-Filho, P. F.; Rodrigues, L. C.; da Silva Dias, C.; Barbosa-Filho, J. M. Brominated Compounds from Marine Sponges of the Genus Aplysina and a Compilation of Their 13C NMR Spectral Data. *Mar. Drugs* **2011**, *9*, 2316−2368.
(35) Lever, J.; Brkljača, R.; Rix, C.; Urban, S. Application of Networking Approaches to Assess the Chemical Diversity, Biogeography, and Pharmaceutical Potential of Verongiida Natural Products. *Mar. Drugs* **2021**, *19*, No. 582.
(36) Moody, K.; Thomson, R. H.; Fattorusso, E.; Minale, L.; Sodano, G. Aerothionin and Homoaerothionin: Two Tetrabromo Spirocyclohexadienylisoxazoles from Verongia Sponges. *J. Chem. Soc., Perkin Trans. 1* **1972**, 18−24.
(37) Peng, J.; Li, J.; Hamann, M. T.The Marine Bromotyrosine Derivatives. In *The Alkaloids: Chemistry and Biology*; Elsevier, 2005; pp 59−262.
(38) Putz, A.; Kloeppel, A.; Pfannkuchen, M.; Brümmer, F.; Proksch, P. Depth-Related Alkaloid Variation in Mediterranean Aplysina Sponges. *Z. Naturforsch., C* **2009**, *64*, 279−287.
(39) Lipowicz, B.; Hanekop, N.; Schmitt, L.; Proksch, P. An Aeroplysinin-1 Specific Nitrile Hydratase Isolated from the Marine Sponge *Aplysina cavernicola*. *Mar. Drugs* **2013**, *11*, 3046−3067.
(40) Xynas, R.; Capon, R. J. Two New Bromotyrosine-Derived Metabolites from an Australian Marine Sponge, *Aplysina* sp. *Aust. J. Chem.* **1989**, *42*, 1427−1433.
(41) Abou-Shoer, M. I.; Shaala, L. A.; Youssef, D. T. A.; Badr, J. M.; Habib, A.-A. M. Bioactive Brominated Metabolites from the Red Sea Sponge *Suberea mollis*. *J. Nat. Prod.* **2008**, *71*, 1464−1467.
(42) Kelly, S.; Jensen, P.; Henkel, T.; Fenical, W.; Pawlik, J. Effects of Caribbean Sponge Extracts on Bacterial Attachment. *Aquat. Microb. Ecol.* **2003**, *31*, 175−182.
(43) Nothias, L.-F.; Petras, D.; Schmid, R.; Dührkop, K.; Rainer, J.; Sarvepalli, A.; Protsyuk, I.; Ernst, M.; Tsugawa, H.; Fleischauer, M.; Aicheler, F.; Aksenov, A. A.; Alka, O.; Allard, P.-M.; Barsch, A.; Cachet, X.; Caraballo-Rodriguez, A. M.; Da Silva, R. R.; Dang, T.; Garg, N.; Gauglitz, J. M.; Gurevich, A.; Isaac, G.; Jarmusch, A. K.; Kameník, Z.; Kang, K. B.; Kessler, N.; Koester, I.; Korf, A.; Le Gouellec, A.; Ludwig, M.; Martin, H. C.; McCall, L.-I.; McSayles, J.; Meyer, S. W.; Mohimani, H.; Morsy, M.; Moyne, O.; Neumann, S.; Neuweger, H.; Nguyen, N. H.; Nothias-Esposito, M.; Paolini, J.; Phelan, V. V.; Pluskal, T.; Quinn, R. A.; Rogers, S.; Shrestha, B.; Tripathi, A.; van der Hooft, J. J. J.; Vargas,

https://doi.org/10.1021/acsomega.2c05415
ACS Omega 2022, 7, 43068−43083

F.; Weldon, K. C.; Witting, M.; Yang, H.; Zhang, Z.; Zubeil, F.; Kohlbacher, O.; Böcker, S.; Alexandrov, T.; Bandeira, N.; Wang, M.; Dorrestein, P. C. Feature-Based Molecular Networking in the GNPS Analysis Environment. *Nat. Methods* **2020**, *17*, 905−908.
(44) DeBose, J.; Paul, V. J. Chemical Signatures of Multi-Species Foraging Aggregations Are Attractive to Fish. *Mar. Ecol.: Prog. Ser.* **2014**, *498*, 243−248.
(45) Berlinck, R. G. S.; Crnkovic, C. M.; Gubiani, J. R.; Bernardi, D. I.; Ióca, L. P.; Quintana-Bulla, J. I. The Isolation of Water-Soluble Natural Products—Challenges, Strategies and Perspectives. *Nat. Prod. Rep.* **2022**, *39*, 596−669.
(46) Cancelada, L.; Torres, R. R.; Luna, J. G.; Dorrestein, P. C.; Aluwihare, L. I.; Prather, K. A.; Petras, D. Assessment of Styrene-divinylbenzene Polymer (PPL) Solid-phase Extraction and Non-targeted Tandem Mass Spectrometry for the Analysis of Xenobiotics in Seawater. *Limnol. Oceanogr.: Methods* **2022**, *20*, 89−101.
(47) Stepan, S. F.; Smith, J. F. Some Conditions for Use of Macroreticular Resins in the Quantitative Analysis of Organic Pollutants in Water. *Water Res.* **1977**, *11*, 339−342.
(48) Thurman, E. M.; Snavely, K. Advances in Solid-Phase Extraction Disks for Environmental Chemistry. *TrAC, Trends Anal. Chem.* **2000**, *19*, 18−26.
(49) Lepane, V. Comparison of XAD Resins for the Isolation of Humic Substances from Seawater. *J. Chromatogr. A* **1999**, *845*, 329−335.
(50) Fiore, C. L.; Freeman, C. J.; Kujawinski, E. B. Sponge Exhalent Seawater Contains a Unique Chemical Profile of Dissolved Organic Matter. *PeerJ* **2017**, *5*, No. e2870.
(51) Olinger, L. K.; Strangman, W. K.; McMurray, S. E.; Pawlik, J. R. Sponges With Microbial Symbionts Transform Dissolved Organic Matter and Take Up Organohalides. *Front. Mar. Sci.* **2021**, *8*, No. 665789.
(52) Nicacio, K. J.; Ióca, L. P.; Fróes, A. M.; Leomil, L.; Appolinario, L. R.; Thompson, C. C.; Thompson, F. L.; Ferreira, A. G.; Williams, D. E.; Andersen, R. J.; Eustaquio, A. S.; Berlinck, R. G. S. Cultures of the Marine Bacterium *Pseudovibrio denitrificans* Ab134 Produce Bromotyrosine-Derived Alkaloids Previously Only Isolated from Marine Sponges. *J. Nat. Prod.* **2017**, *80*, 235−240.
(53) Dührkop, K.; Nothias, L.-F.; Fleischauer, M.; Reher, R.; Ludwig, M.; Hoffmann, M. A.; Petras, D.; Gerwick, W. H.; Rousu, J.; Dorrestein, P. C.; Böcker, S. Systematic Classification of Unknown Metabolites Using High-Resolution Fragmentation Mass Spectra. *Nat. Biotechnol.* **2021**, *39*, 462−471.
(54) Pawlik, J. R.; McMurray, S. E. The Emerging Ecological and Biogeochemical Importance of Sponges on Coral Reefs. *Annu. Rev. Mar. Sci.* **2020**, *12*, 315−337.
(55) Pluskal, T.; Castillo, S.; Villar-Briones, A.; Orešič, M. MZmine 2: Modular Framework for Processing, Visualizing, and Analyzing Mass Spectrometry-Based Molecular Profile Data. *BMC Bioinf.* **2010**, *11*, No. 395.
(56) Shannon, P.; Markiel, A.; Ozier, O.; et al. Cytoscape: A Software Environment for Integrated Models of Biomolecular Interaction Networks. *Genome Res.* **2003**, *13*, 2498−2504.
(57) Wang, M.; Carver, J. J.; Phelan, V. V.; Sanchez, L. M.; Garg, N.; Peng, Y.; Nguyen, D. D.; Watrous, J.; Kapono, C. A.; Luzzatto-Knaan, T.; Porto, C.; Bouslimani, A.; Melnik, A. V.; Meehan, M. J.; Liu, W.-T.; Crüsemann, M.; Boudreau, P. D.; Esquenazi, E.; Sandoval-Calderón, M.; Kersten, R. D.; Pace, L. A.; Quinn, R. A.; Duncan, K. R.; Hsu, C.-C.; Floros, D. J.; Gavilan, R. G.; Kleigrewe, K.; Northen, T.; Dutton, R. J.; Parrot, D.; Carlson, E. E.; Aigle, B.; Michelsen, C. F.; Jelsbak, L.; Sohlenkamp, C.; Pevzner, P.; Edlund, A.; McLean, J.; Piel, J.; Murphy, B. T.; Gerwick, L.; Liaw, C.-C.; Yang, Y.-L.; Humpf, H.-U.; Maansson, M.; Keyzers, R. A.; Sims, A. C.; Johnson, A. R.; Sidebottom, A. M.; Sedio, B. E.; Klitgaard, A.; Larson, C. B.; Boya, P. C. A.; Torres-Mendoza, D.; Gonzalez, D. J.; Silva, D. B.; Marques, L. M.; Demarque, D. P.; Pociute, E.; O'Neill, E. C.; Briand, E.; Helfrich, E. J. N.; Granatosky, E. A.; Glukhov, E.; Ryffel, F.; Houson, H.; Mohimani, H.; Kharbush, J. J.; Zeng, Y.; Vorholt, J. A.; Kurita, K. L.; Charusanti, P.; McPhail, K. L.; Nielsen, K. F.; Vuong, L.; Elfeki, M.; Traxler, M. F.; Engene, N.; Koyama, N.; Vining, O. B.; Baric, R.; Silva, R. R.; Mascuch, S. J.; Tomasi, S.; Jenkins, S.; Macherla, V.; Hoffman, T.; Agarwal, V.; Williams, P. G.; Dai, J.; Neupane, R.; Gurr, J.; Rodríguez, A. M. C.; Lamsa, A.; Zhang, C.; Dorrestein, K.; Duggan, B. M.; Almaliti, J.; Allard, P.-M.; Phapale, P.; Nothias, L.-F.; Alexandrov, T.; Litaudon, M.; Wolfender, J.-L.; Kyle, J. E.; Metz, T. O.; Peryea, T.; Nguyen, D.-T.; VanLeer, D.; Shinn, P.; Jadhav, A.; Müller, R.; Waters, K. M.; Shi, W.; Liu, X.; Zhang, L.; Knight, R.; Jensen, P. R.; Palsson, B. Ø.; Pogliano, K.; Linington, R. G.; Gutiérrez, M.; Lopes, N. P.; Gerwick, W. H.; Moore, B. S.; Dorrestein, P. C.; Bandeira, N. Sharing and Community Curation of Mass Spectrometry Data with Global Natural Products Social Molecular Networking. *Nat. Biotechnol.* **2016**, *34*, 828−837.
(58) Gunasekera, M.; Gunasekera, P. S. Dihydroxyaerothionin and Aerophobin 1. Two Brominated Tyrosine Metabolites from the Deep Water Marine Sponge *Verongula rigida*. *J. Nat. Prod.* **1989**, *52*, 753−756.
(59) Cimino, G.; De Rosa, S.; De Stefano, S.; Self, R.; Sodano, G. The Bromo-Compounds of the True Sponge *Verongia aerophoba*. *Tetrahedron Lett.* **1983**, *24*, 3029−3032.
(60) Rodríguez, A. D.; Piña, I. C. The Structures of Aplysinamisines I, II, and III: New Bromotyrosine-Derived Alkaloids from the Caribbean Sponge *Aplysina cauliformis*. *J. Nat. Prod.* **1993**, *56*, 907−914.
(61) Ciminiello, P.; Dell'Aversano, C.; Fattorusso, E.; Magno, S. Archerine, a Novel Anti Histaminic Bromotyrosine-Derived Compound from the Caribbean Marine Sponge *Aplysina archeri*. *Eur. J. Org. Chem.* **2001**, 55−60.
(62) Schymanski, E. L.; Jeon, J.; Gulde, R.; Fenner, K.; Ruff, M.; Singer, H. P.; Hollender, J. Identifying Small Molecules via High Resolution Mass Spectrometry: Communicating Confidence. *Environ. Sci. Technol.* **2014**, *48*, 2097−2098.
(63) Salib, M. N.; Jamison, M. T.; Molinski, T. F. Bromo-Spiroisoxazoline Alkaloids, Including an Isoserine Peptide, from the Caribbean Marine Sponge *Aplysina lacunosa*. *J. Nat. Prod.* **2020**, *83*, 1532−1540.
(64) Ragini, K.; Fromont, J.; Piggott, A. M.; Karuso, P. Enantiodivergence in the Biosynthesis of Bromotyrosine Alkaloids from Sponges? *J. Nat. Prod.* **2017**, *80*, 215−219.
(65) Grimblat, N.; Zanardi, M. M.; Sarotti, A. M. Beyond DP4: An Improved Probability for the Stereochemical Assignment of Isomeric Compounds Using Quantum Chemical Calculations of NMR Shifts. *J. Org. Chem.* **2015**, *80*, 12526−12534.
(66) Bhavaraju, S.; Taylor, D.; Niemitz, M.; Lankin, D. C.; Bzhelyansky, A.; Giancaspro, G. I.; Liu, Y.; Pauli, G. F. NMR-Based Quantum Mechanical Analysis Builds Trust and Orthogonality in Structural Analysis: The Case of a Bisdesmosidic Triglycoside as Withania Somnifera Aerial Parts Marker. *J. Nat. Prod.* **2021**, *84*, 836−845.
(67) Choules, M. P.; Bisson, J.; Gao, W.; Lankin, D. C.; McAlpine, J. B.; Niemitz, M.; Jaki, B. U.; Franzblau, S. G.; Pauli, G. F. Quality Control of Therapeutic Peptides by ^{1}H NMR HiFSA Sequencing. *J. Org. Chem.* **2019**, *84*, 3055−3073.
(68) Tilvi, S.; Majik, M. S.; Singh, K. S. Mass Spectrometry for Determination of Bioactive Compounds. In *Comprehensive Analytical Chemistry*; Elsevier, 2014; Vol. *65*, pp 193−218.
(69) Wang, F.; Liigand, J.; Tian, S.; Arndt, D.; Greiner, R.; Wishart, D. S. CFM-ID 4.0: More Accurate ESI-MS/MS Spectral Prediction and Compound Identification. *Anal. Chem.* **2021**, *93*, 11692−11700.
(70) Sorokina, M.; Merseburger, P.; Rajan, K.; Yirik, M. A.; Steinbeck, C. COCONUT Online: Collection of Open Natural Products Database. *J. Cheminf.* **2021**, *13*, No. 2.
(71) Hastings, J.; Owen, G.; Dekker, A.; Ennis, M.; Kale, N.; Muthukrishnan, V.; Turner, S.; Swainston, N.; Mendes, P.; Steinbeck, C. ChEBI in 2016: Improved Services and an Expanding Collection of Metabolites. *Nucleic Acids Res.* **2016**, *44*, D1214−D1219.
(72) Carney, J. R.; Rinehart, K. L. Biosynthesis of Brominated Tyrosine Metabolites by *Aplysina fistularis*. *J. Nat. Prod.* **1995**, *58*, 971−985.

https://doi.org/10.1021/acsomega.2c05415
ACS Omega 2022, 7, 43068−43083

(73) Chang, C. W. J.; Weinheimer, A. J. 2-Hydroxy, 3,5-Dibromo, 4-Methoxyphenylacetamide, a Dibromotyrosine Metabolite from *Psammoposilla purpurea*. *Tetrahedron Lett.* **1977**, *18*, 4005−4007.
(74) Shaala, L. A.; Khalifa, S. I.; Mesbah, M. K.; Van Soest, R. W. M.; Youssef, D. T. A. Subereaphenol A, a New Cytotoxic and Antimicrobial Dibrominated Phenol from the Red Sea Sponge *Suberea mollis*. *Nat. Prod. Commun.* **2008**, *3*, 219−222.
(75) Cruz, F.; Quijano, L.; Gómez-Garibay, F.; Rios, T. Brominated Metabolites from the Sponge *Aplysina (verongia) thiona*. *J. Nat. Prod.* **1990**, *53*, 543−548.
(76) Minale, L.; Sodano, G.; Chen, W. R.; Chan, A. M. Aeroplysinin-2, a Dibromolactone from Marine Sponges *Aplysina (verongia) aerophoba* and *Ianthella* sp. *J. Chem. Soc., Chem. Commun.* **1972**, *11*, 674−675.
(77) Pauli, G. F.; Chen, S.-N.; Simmler, C.; Lankin, D. C.; Gödecke, T.; Jaki, B. U.; Friesen, J. B.; McAlpine, J. B.; Napolitano, J. G. Importance of Purity Evaluation and the Potential of Quantitative ^{1}H NMR as a Purity Assay: Miniperspective. *J. Med. Chem.* **2014**, *57*, 9220−9231.
(78) Myers, O. D.; Sumner, S. J.; Li, S.; Barnes, S.; Du, X. One Step Forward for Reducing False Positive and False Negative Compound Identifications from Mass Spectrometry Metabolomics Data: New Algorithms for Constructing Extracted Ion Chromatograms and Detecting Chromatographic Peaks. *Anal. Chem.* **2017**, *89*, 8696−8703.
(79) Marenich, A. V.; Cramer, C. J.; Truhlar, D. G. Universal Solvation Model Based on Solute Electron Density and on a Continuum Model of the Solvent Defined by the Bulk Dielectric Constant and Atomic Surface Tensions. *J. Phys. Chem. B* **2009**, *113*, 6378−6396.
(80) Kaupp, M.; Malkina, O. L.; Malkin, V. G. Interpretation of ^{13}C NMR Chemical Shifts in Halomethyl Cations. On the Importance of Spin-Orbit Coupling and Electron Correlation. *Chem. Phys. Lett.* **1997**, *265*, 55−59.

https://doi.org/10.1021/acsomega.2c05415
ACS Omega 2022, 7, 43068−43083